



# Paleoceanography and Paleoclimatology

## RESEARCH ARTICLE

10.1029/2018PA003353

### Key Points:

- High-resolution Cape Basin XRF Ca/Ti records mostly reflect changes in deep water carbonate ion saturation during the last four glacial cycles
- Low-frequency XRF Ca/Ti variations indicate the effects of carbonate compensation and/or changes in deep ocean respired carbon content
- High-frequency XRF Ca/Ti variations suggest fast changes in the redistribution of carbonate ions in the Atlantic Ocean via the AMOC

### Supporting Information:

- Supporting Information S1

### Correspondence to:

J. Gottschalk,  
jgottsch@ldeo.columbia.edu

### Citation:

Gottschalk, J., Hodell, D. A., Skinner, L. C., Crowhurst, S. J., Jaccard, S. L., & Charles, C. (2018). Past carbonate preservation events in the deep Southeast Atlantic Ocean (Cape Basin) and their implications for Atlantic overturning dynamics and marine carbon cycling. *Paleoceanography and Paleoclimatology*, 33. <https://doi.org/10.1029/2018PA003353>

Received 6 MAR 2018

Accepted 4 JUN 2018

Accepted article online 11 JUN 2018

## Past Carbonate Preservation Events in the Deep Southeast Atlantic Ocean (Cape Basin) and Their Implications for Atlantic Overturning Dynamics and Marine Carbon Cycling

Julia Gottschalk<sup>1,2,3</sup> , David A. Hodell<sup>1</sup> , Luke C. Skinner<sup>1</sup> , Simon J. Crowhurst<sup>1</sup>, Samuel L. Jaccard<sup>2</sup> , and Christopher Charles<sup>4</sup>

<sup>1</sup>Godwin Laboratory for Palaeoclimate Research, Earth Sciences Department, University of Cambridge, Cambridge, UK,

<sup>2</sup>Institute of Geological Sciences and Oeschger Center for Climate Change Research, University of Bern, Bern, Switzerland,

<sup>3</sup>Now at Lamont-Doherty-Earth-Observatory, Columbia University, Palisades, NY, USA, <sup>4</sup>Scripps Institute of Oceanography, University of California, San Diego, La Jolla, CA, USA

**Abstract** Micropaleontological and geochemical analyses reveal distinct millennial-scale increases in carbonate preservation in the deep Southeast Atlantic (Cape Basin) during strong and prolonged Greenland interstadials that are superimposed on long-term (orbital-scale) changes in carbonate burial. These data suggest carbonate oversaturation of the deep Atlantic and a strengthened Atlantic Meridional Overturning Circulation (AMOC) during the most intense Greenland interstadials. However, proxy evidence from outside the Cape Basin indicates that AMOC changes also occurred during weaker and shorter Greenland interstadials. Here we revisit the link between AMOC dynamics and carbonate saturation in the deep Cape Basin over the last 400 kyr (sediment cores TN057-21, TN057-10, and Ocean Drilling Program Site 1089) by reconstructing centennial changes in carbonate preservation using millimeter-scale X-ray fluorescence (XRF) scanning data. We observe close agreement between variations in XRF Ca/Ti, sedimentary carbonate content, and foraminiferal shell fragmentation, reflecting a common control primarily through changing deep water carbonate saturation. We suggest that the high-frequency (suborbital) component of the XRF Ca/Ti records indicates the fast and recurrent redistribution of carbonate ions in the Atlantic basin via the AMOC during both long/strong and short/weak North Atlantic climate anomalies. In contrast, the low-frequency (orbital) XRF Ca/Ti component is interpreted to reflect slow adjustments through carbonate compensation and/or changes in the deep ocean respired carbon content. Our findings emphasize the recurrent influence of rapid AMOC variations on the marine carbonate system during past glacial periods, providing a mechanism for transferring the impacts of North Atlantic climate anomalies to the global carbon cycle via the Southern Ocean.

## 1. Introduction

The burial and preservation of calcium carbonate (CaCO<sub>3</sub>) in marine sediments both play an important role in the global carbon cycle (Archer & Maier-Reimer, 1994; Berger & Keir, 1984; Boyle, 1988b; Broecker & Peng, 1987; Heinze et al., 1991; Sigman & Boyle, 2000). Although the preservation of carbonate in the ocean is depth dependent, it is preserved to deeper depths in the Atlantic because of the proximity to the formation sites of relatively high [CO<sub>3</sub><sup>2-</sup>] North Atlantic Deep Water (NADW; Archer, 1996). In contrast to NADW, which is slightly supersaturated with respect to CaCO<sub>3</sub> (Key et al., 2004), southern sourced water masses such as Antarctic Bottom Water (AABW) and Circumpolar Deep Water (CDW) are undersaturated with respect to CaCO<sub>3</sub> owing to elevated concentrations of dissolved inorganic carbon (DIC) from the respiration of organic carbon (Key et al., 2004; Figure 1). These southern sourced water masses therefore tend to be corrosive, and thus promote CaCO<sub>3</sub> dissolution. The depth of the lysocline, below which marine carbonates begin to be thermodynamically unstable, and are hence significantly affected by dissolution (Biscaye et al., 1977), corresponds in the deep Atlantic roughly to the mixing zone between northern and southern sourced water masses (Broecker & Peng, 1989; Henrich et al., 2003; Thunell, 1982). Past changes in the location of the lysocline and/or the carbonate compensation depth (CCD), below which dissolution of biogenic carbonates is nearly complete, should therefore reflect reorganizations of the ocean circulation and changes in the global ocean carbonate system.

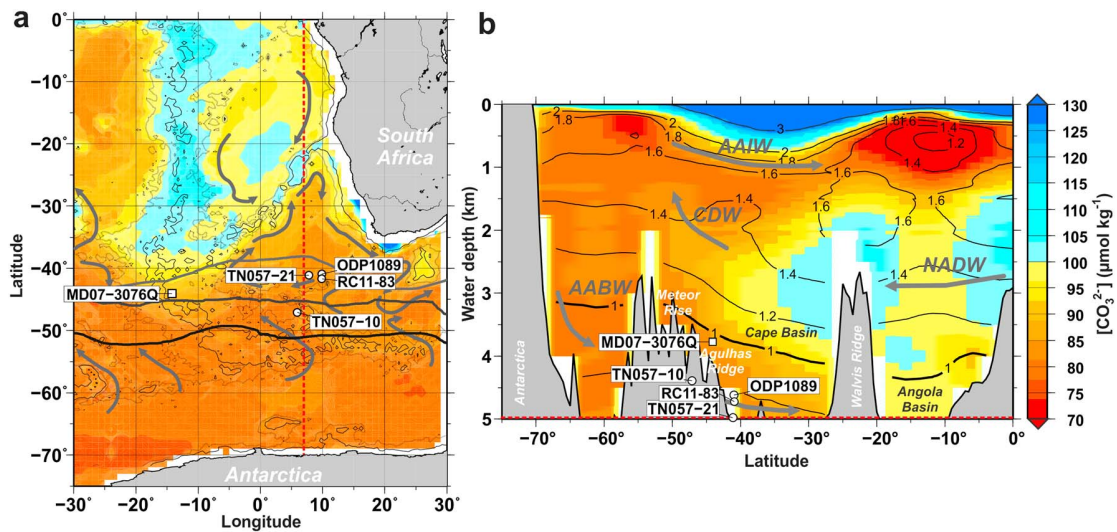


**Figure 1.** Location of the study cores. (a) Carbonate ion concentrations ( $[\text{CO}_3^{2-}]$ ) in bottom waters in the Southeast Atlantic (Key et al., 2004), thin line tracks the 4- (stippled) and 2-km isobaths (solid); the position of major fronts are shown in dark gray (Polar Front), in gray (Sub-Antarctic Front), and in light gray (Sub-Tropical Front; Orsi et al., 1995; Sokolov & Rintoul, 2009); deep ocean currents are shown after Tucholke and Embley (1984) and Stramma and England (1999). (b) Meridional transect of  $[\text{CO}_3^{2-}]$  (shaded) and calcite saturation  $\Omega = [\text{CO}_3^{2-}]_{\text{in-situ}}/[\text{CO}_3^{2-}]_{\text{saturated}}$  (contoured) along 7°E (Key et al., 2004). Circles indicate the location of the study cores from the Cape Basin, and square shows sediment core used for comparison (Table S1). Deep water masses are indicated according to Talley (2013; AABW: Antarctic Bottom Water, NADW: North Atlantic Deep Water, CDW: Circumpolar Deep Water, AAIW: Antarctic Intermediate Water).

On glacial-interglacial time scales, sedimentary carbonate preservation in the deep ocean is significantly influenced by changes in the overall oceanic DIC and alkalinity inventories, which in turn impact on atmospheric  $\text{CO}_2$  levels via variations of the global net air-sea  $\text{CO}_2$  flux (Archer & Maier-Reimer, 1994; Boyle, 1988b; Broecker & Peng, 1987; Ridgwell & Zeebe, 2005). Any changes in the ocean's DIC and alkalinity content that impact on the global average carbonate saturation state will tend to be restored (i.e., eliminated) by adjustments in the position of the lysocline (and possibly the CCD), which is referred to as "carbonate compensation" (Broecker, 1982; Broecker & Peng, 1987; Sigman et al., 1998). Over millennial time scales, the distinct chemical signatures of northern versus southern sourced water masses make sedimentary carbonate preservation specifically in the South Atlantic primarily dependent on prevailing ocean circulation patterns that may have shifted rapidly in the past (Gottschalk et al., 2015; Henry et al., 2016; Keigwin & Jones, 1994; McManus et al., 2004), with implications for atmospheric  $\text{CO}_2$  levels (e.g., Bouttes et al., 2012; Schmittner & Galbraith, 2008). The sedimentary carbonate record of the deep Atlantic hence integrates the influence of various ocean processes that operate on different time scales (Hodell et al., 2001).

The patterns of deep Atlantic and Pacific carbonate preservation differ over glacial-interglacial time scales. During glacial periods (in particular, the late stage), carbonate is generally well preserved in the deep Pacific, whereas in the deep Atlantic carbonate burial was influenced by dissolution (Balsam & McCoy, 1987; Crowley, 1985; Farrell & Prell, 1989; Hodell et al., 2001; Howard & Prell, 1994). Interglacial periods (again, the late stage especially) show enhanced dissolution in the Pacific (Farrell & Prell, 1989; Le & Shackleton, 1992), whereas carbonate was generally preserved in the Atlantic Ocean during these times (Hodell et al., 2001). The "Pacific-type" carbonate preservation is believed to mainly reflect adjustments of the lysocline and the CCD to maintain alkalinity balance between riverine input and marine carbonate burial (Hodell et al., 2001; Kerr et al., 2017). This is supported by relatively small bottom water  $[\text{CO}_3^{2-}]$  variations observed in the Pacific over glacial-interglacial transitions ( $\sim 15 \mu\text{mol/kg}$ ), suggesting an effective carbonate ion buffering (Anderson & Archer, 2002; de la Fuente et al., 2017; Kerr et al., 2017; Marchitto et al., 2005; Yu, Anderson, et al., 2013). The Atlantic-type carbonate preservation signal results mainly from changes in the formation and export of NADW (Broecker & Clark, 2001; Hodell et al., 2001; Howard & Prell, 1994). This is supported by contrasting carbonate preservation signals in the deep and shallow Atlantic: widespread carbonate dissolution occurred in the last glacial in the deep Atlantic, which was occupied by predominantly southern sourced water masses (Bickert & Wefer, 1996; Gottschalk et al., 2015; Hodell et al., 2001; Howard & Prell, 1994; Yu et al., 2008), while enhanced carbonate preservation

was found at shallower depths that were occupied by Glacial North Atlantic Intermediate Water (GNAIW; Haddad & Droxler, 1996; Henrich et al., 2003; Wall-Palmer et al., 2012). The coevolution of changes in carbonate dissolution with AMOC variability in the glacial Atlantic underlines its primary association with water mass dynamics (and the evolving geochemical signatures of deep water end-members) rather than whole-ocean adjustments to an imbalance in the DIC and alkalinity inventories. However, the exact timing and interplay of these two (Atlantic and Pacific) components in driving the deep ocean carbonate chemistry during past glacial-interglacial cycles remains insufficiently documented and understood.

Here we present high-resolution (millimeter-scale) XRF Ca/Ti records over the last four glacial cycles from marine sediment cores TN057-21 (41.08°S, 7.49°E; 4,981-m water depth), TN057-10 (47.10°S, 5.92°E; 4,390-m water depth), and from Ocean Drilling Program (ODP) Site 1089 (40.94°S, 9.89°E; 4,624-m water depth) retrieved from the deep Cape Basin. Our core sites are located below the modern lysocline and are sensitive to changes in carbonate saturation. Variations in the XRF Ca/Ti ratios in our study cores show excellent agreement with changes in coulometrically determined carbonate weight percentages, which given the limitations from bioturbation provide therefore a centennially resolved record of carbonate content variability in the deep Cape Basin during the last 400 kyr. Complementary analyses of planktic foraminifer fragmentation and indicators of water mass provenance in sediment core TN057-21 emphasize that they largely reflect fluctuations in the preservation of carbonate owing to changes in the corrosiveness of bottom and/or pore waters in the Southeast Atlantic, although the influence from sedimentation rate changes cannot be ruled out. We investigate the impact of whole-ocean mass balance processes and transient circulation changes on carbonate (i.e., calcite) saturation in the deep Cape Basin during the last glacial period (sediment cores TN057-21 and TN057-10) and beyond the last glacial cycle (ODP Site 1089) and assess its temporal relation to Northern Hemisphere climate anomalies and atmospheric CO<sub>2</sub> variations.

## 2. Study Area

### 2.1. Core Locations

Piston core TN057-21 is located in the southern Cape Basin north of the Agulhas Ridge (Figure 1) and was collected on a sediment drift, where deep currents focus sediments eroded in the northern and eastern Cape Basin (Tucholke & Embley, 1984). Consequently, average sedimentation rates at the core site are high (~14 cm/kyr; section 3.5). The 13.84-m long core extends back to Marine Isotope Stage (MIS) 5a.

ODP Site 1089 is located at a sediment drift north of the Agulhas Ridge, within 200 km of TN057-21 (Figure 1). High sedimentation rates similar to those observed in TN057-21 prevailed at this site throughout the last four glacial-interglacial cycles (~15 cm/kyr on average; section 3.5). Both TN057-21 and ODP Site 1089 are located within the modern sub-Antarctic Zone (Figure 1a).

Piston core TN057-10 was retrieved from the western flank of the Meteor Rise. The 13.2-m piston core (TN057-10-PC3) and 2.2-m trigger core (TN057-10-TC3) span the last ~100 kyr with an average sedimentation rate of ~11 cm/kyr (Hodell et al., 2000). The trigger core captured the sediment-water interface, which was lost during coring from piston core TN057-10. We have produced a composite record combining the top of the trigger core with the piston core by splicing the planktic  $\delta^{18}\text{O}$  records from the individual cores. The depth scale of piston core TN057-10 was therefore shifted by 30.6 cm. TN057-10 is located within the modern sub-Antarctic Zone (Figure 1a).

### 2.2. Carbonate Chemistry in the Deep Cape Basin

The study sites are presently bathed in low-[CO<sub>3</sub><sup>2-</sup>] Antarctic Bottom Water (AABW), which is characterized by calcite undersaturation ( $\Omega < 1$ ; Figure 1 and supporting information Table S1). Based on calculations using the CO<sub>2</sub>SYS program (Lewis & Wallace, 1998) and input parameters from the World Ocean Atlas 2009 and the GLODAP database (Antonov et al., 2010; Key et al., 2004; Locarnini et al., 2010), the carbonate ion saturation at our core sites ( $\Delta[\text{CO}_3^{2-}] = [\text{CO}_3^{2-}]_{\text{in situ}} - [\text{CO}_3^{2-}]_{\text{saturated}}$ ) ranges between  $-27.8 \mu\text{mol/kg}$  at the deepest site (TN057-21) to  $-20.3 \mu\text{mol/kg}$  at our shallowest site (TN057-10; supporting information Table S1). The transition from carbonate oversaturation to undersaturation ( $\Omega = 1$ ) is located ~1 km above our core sites and coincides with the transition zone between low-[CO<sub>3</sub><sup>2-</sup>] southern sourced AABW and high-[CO<sub>3</sub><sup>2-</sup>] northern sourced NADW (Figure 1).

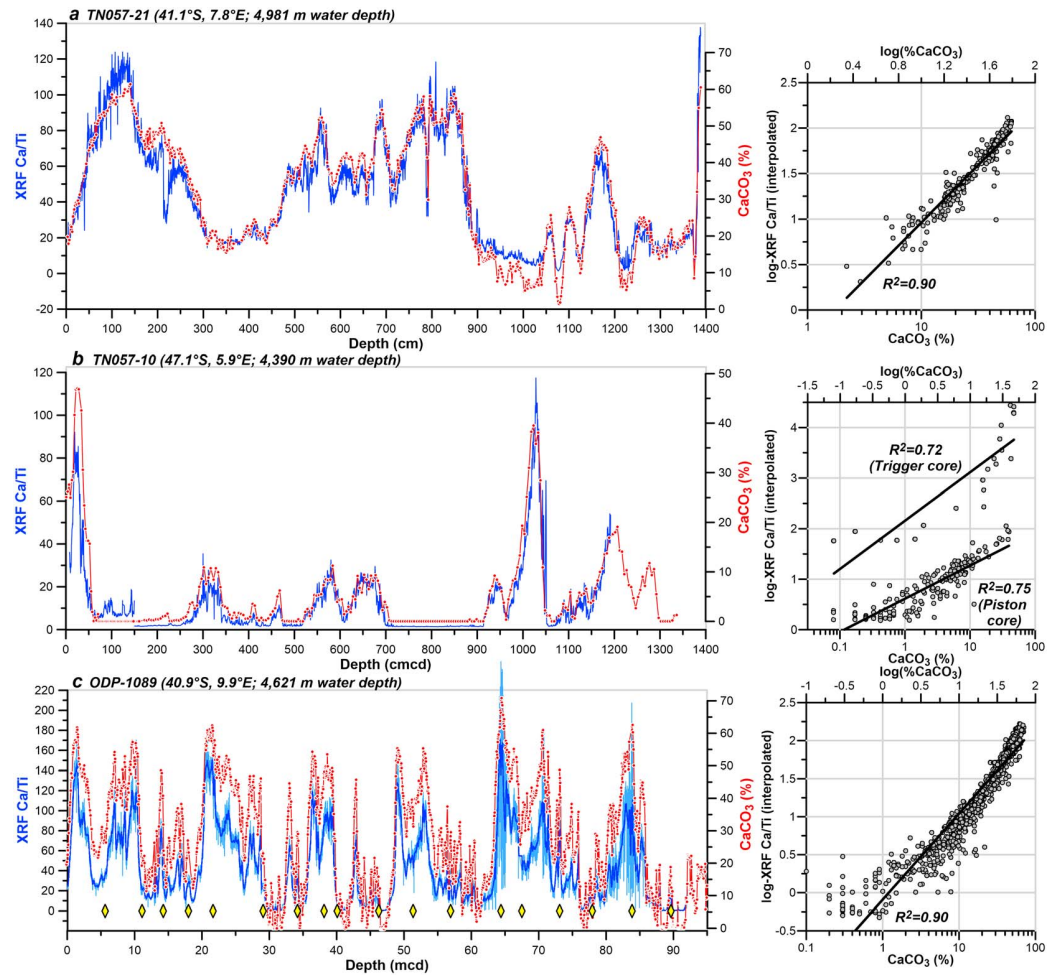


**Figure 2.** Comparison of downcore variations of carbonate weight percentages (red) and the XRF Ca/Ti ratios (blue) in (a) TN057-21, (b) TN057-10, and for (c) ODP Site 1089 (light blue: original data, blue: 50 point-running average, yellow symbols: splice breaks); right panels show cross plots between carbonate weight percentages (on a logarithmic scale) and log-XRF Ca/Ti values interpolated onto the carbonate data (at ODP Site 1089: a 50-point running average was applied to the XRF Ca/Ti data prior to interpolation). Note that XRF ratios in TN057-10 are slightly offset between the trigger and piston core due to slight differences in the XRF deconvolution, likely caused by different scanning geometries of the u-channels.

### 3. Methods

#### 3.1. Carbonate Content

The weight percentage of carbonate was determined from discrete samples shortly after core recovery by coulometric titration using a 5011 CO<sub>2</sub> coulometer (UIC Inc.) with an automatic AutoMate FX acidification preparation system (Engleman et al., 1985). In total, ~600 discrete samples were analyzed in sediment core TN057-21 (every 2 cm; Sachs & Anderson, 2003), ~1,800 samples at ODP Site 1089 (Hodell et al., 2001, 2003), and ~300 samples in TN057-10 (both every 5 cm; Channell et al., 2000; Kanfoush et al., 2000; Figure 2). The carbonate data of TN057-21 of Sachs and Anderson (2003) were determined after minor, yet significant, core shrinkage. Their reported depth scale was adjusted to be consistent with the original depth scale reported in the cruise report (supporting information Table S2). Analytical precision was estimated by analysis of reagent-grade carbonate (100%) standards that yielded a mean and standard deviation (1σ) of 99.97 ± 0.82%.

#### 3.2. High-Resolution X-Ray Fluorescence (XRF) Core Scanning

XRF scanning of sediment core surfaces is a rapid and nondestructive method for a semiquantitative determination of variations in elemental composition and was performed using a third-generation Avaatech® XRF

core scanner at the University of Cambridge on u-channels sampled from sediment cores TN057-21, TN057-10, and ODP Site 1089, which were originally taken for paleomagnetic analysis (Channell et al., 2000; Stoner et al., 2003; Figure 2). XRF data were obtained downcore every 2.5 mm. The cores were measured using a current of 0.2 mA at 10 kV with no filter, at 30 kV using a thin Pb filter, and at 50 kV using a Cu filter. Integration time was 40 s. Shrinkage of sediments in the u-channels owing to dehydration was identified by visual inspection of the sediments and comparison against the XRF data (assuming that voids result in a synchronized decline in the counts of the sum of all elements). Corrections were then made by correlating the XRF Ca/Ti ratios to the discrete measurements of carbonate weight percentages in the sediment cores at and near sediment cracks.

### 3.3. Sedimentary Census Counts

Samples from the entire sediment sequence of TN057-21 (every 2 cm) were washed through a 63  $\mu\text{m}$  sieve and oven dried at 40°C. Sediment grains including planktic foraminifera and fragments (smaller than half a shell) were counted from sediment splits of the  $>150 \mu\text{m}$  size fraction until approximately 300 whole planktic foraminifer tests were counted (results were in part published previously; Barker & Diz, 2014). The fragmentation index was calculated according to Howard and Prell (1994). The depth scale of data reported by Barker and Diz (2014) was adjusted to the originally reported depth scale for consistency (supporting information Table S2).

### 3.4. Stable Isotopes

Stable oxygen isotope analyses for TN057-21 and for ODP Site 1089 were performed on *Globigerina bulloides* handpicked from the 250–425- $\mu\text{m}$  size fraction on a Finnigan MAT 252 mass spectrometer (Mortyn et al., 2002, 2003). In TN057-21, a higher-resolution *G. bulloides* stable isotope record was obtained by Barker and Diz (2014) using a narrower *G. bulloides* size fraction (250–300  $\mu\text{m}$ ; Figure 3). Stable oxygen isotope analyses in TN057-10 were made on *Neogloboquadrina pachyderma* (sinistral-coiling) handpicked from the  $>150\text{-}\mu\text{m}$  fraction on VG Isogas (Micromass) Precision Isotope Ratio Mass Spectrometer (Hodell et al., 2000). The data are reported in  $\delta$ -notation with reference to the international Vienna Pee Dee Belemnite (VPDB) standard. The mean external reproducibility of carbonate standards was always better than 0.1 ‰ for  $\delta^{18}\text{O}$  and  $\delta^{13}\text{C}$ .

### 3.5. Chronology

Decreases in planktic  $\delta^{18}\text{O}$  in the Cape Basin have been proposed to coincide with Antarctic warming, as both likely responded to changes in atmospheric air temperatures (Charles et al., 1996; Mortyn et al., 2003). Barker et al. (2009) highlighted sea surface temperature variations of 2–4°C in the Cape Basin during past millennial-scale climate events based on *G. bulloides* Mg/Ca ratios from TN057-21, which would alone explain a large proportion of the observed planktic  $\delta^{18}\text{O}$  variability (Figure 3). However, planktic  $\delta^{18}\text{O}$  can also be influenced by changes in seawater salinity, for instance, due to the influence of local meltwater fluxes and global sea level changes. The influence of meltwater fluxes in the Cape Basin was suggested to be strongest during peak Antarctic warming (Kanfoush et al., 2000), and global sea level changes likely covaried with Antarctic temperature variations (Grant et al., 2012; Siddall et al., 2008). This suggests that seawater salinity changes likely modulated the surface temperature-driven planktic  $\delta^{18}\text{O}$  record with a timing similar to Antarctic temperature variability. To establish a chronology for our study cores, we have therefore correlated the high-resolution *G. bulloides*  $\delta^{18}\text{O}$  of TN057-21 of Barker and Diz (2014) to air temperature changes recorded in  $\delta^{18}\text{O}$  variations of the EPICA Dronning Maud Land (EDML) ice core (EPICA Community Members, 2006), using the newest AICC2012 age scale (Bazin et al., 2013; Veres et al., 2013; Figure 4). Tie points are primarily selected at climatic transitions, and half of the duration of the transition is considered as  $2\sigma$  uncertainty of the chosen tie point. Age-depth markers are complemented by available calibrated  $^{14}\text{C}$  ages for core TN057-21 and RC11-83 that were transferred to TN057-21 by correlating the individual carbonate records (Barker et al., 2009). We also assign a modern age (0 kyr) to the top of core TN057-21 (0 cm), because it cannot be more precisely dated (i.e., using  $^{14}\text{C}$ ) owing to the scarcity of planktic foraminifera. The final age-depth relationship is based on linear interpolation between tie points (Figure 4 and supporting information Table S3).

Chronological uncertainties were determined based on Monte Carlo simulations with the Bayesian statistical software BChron (Haslett & Parnell, 2008), which simulates a large number of statistically supported core chronologies based on the predefined age-depth markers and their uncertainties. For TN057-21, the resulting average  $2\sigma$  uncertainty of the alignment is  $1,000 \pm 500$  years.

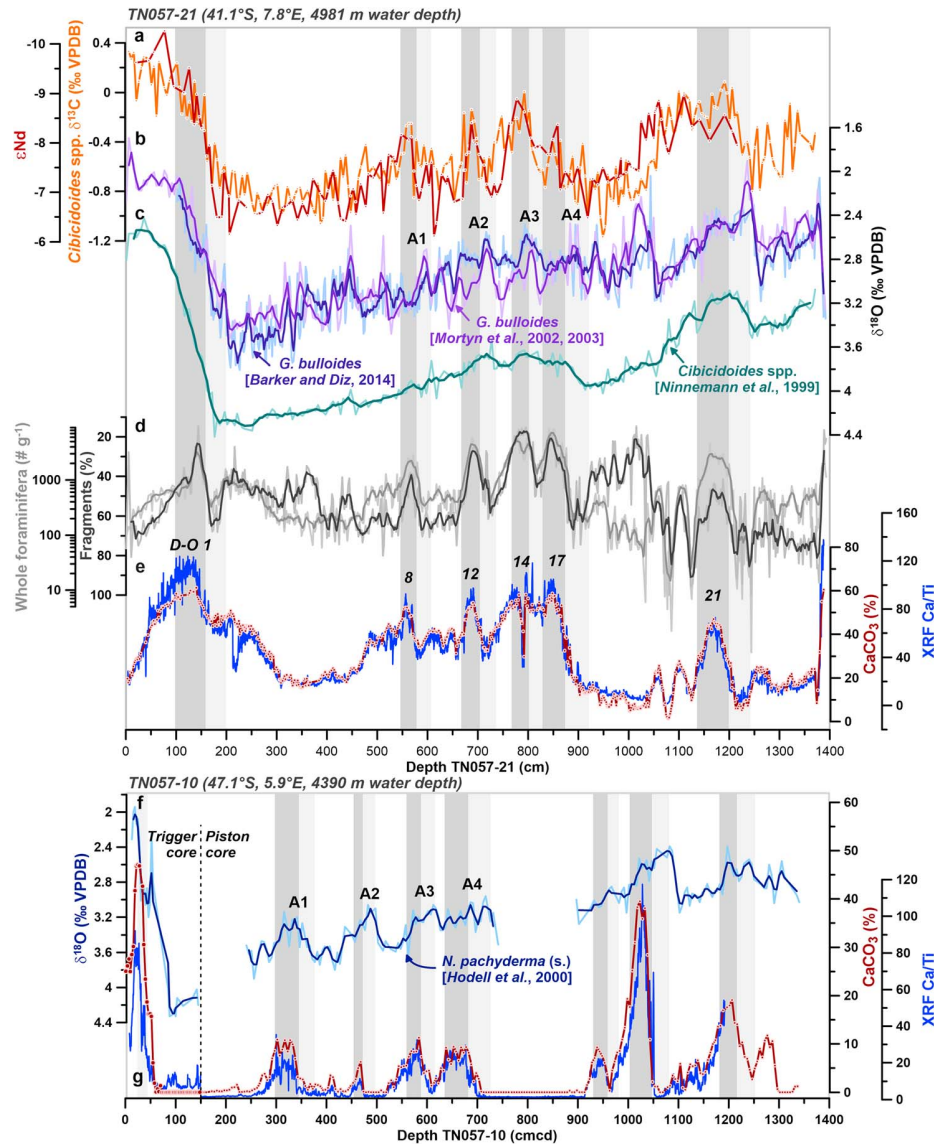


**Figure 3.** Millennial-scale changes in the carbonate chemistry of the deep Cape Basin during the last glacial cycle recorded in (top) TN057-21 and (bottom) TN057-10. (a) *Cibicoides* spp.  $\delta^{13}\text{C}$  (orange; Ninnemann et al., 1999) and water mass source indicator  $\epsilon_{\text{Nd}}$  (dark red; Piotrowski et al., 2008, 2012), (b) *G. bulloides*  $\delta^{18}\text{O}$  data of Mortyn et al. (2002, 2003; purple) and Barker and Diz (2014; blue, depth scale adjusted), (c) *Cibicoides* spp.  $\delta^{18}\text{O}$  (light green; Ninnemann et al., 1999), (d) number of whole planktic foraminifera per gram sediment (light gray; Barker & Diz, 2014) and planktic foraminifer fragmentation (dark gray), (e) coulometrically determined carbonate content (red, depth scale adjusted; Sachs & Anderson, 2003) and the XRF Ca/Ti ratio (blue), (f) *N. pachyderma* (s.)  $\delta^{18}\text{O}$  (Hodell et al., 2000), and (g) coulometrically determined carbonate content (red; Channell et al., 2000; Kanfoush et al., 2000) and the XRF Ca/Ti ratio (blue). Light gray bars highlight decreases and/or minima in planktic  $\delta^{18}\text{O}$ , that is, phases of surface warming that have likely paralleled Antarctic warming events (A1-A4; numbering after Blunier & Brook, 2001). Dark gray bars highlight intervals of pronounced carbonate preservation that coincide with strong and prolonged Dansgaard-Oeschger (D-O, numbering after Dansgaard et al., 1993) interstadials.

Our chronology results in a good agreement between the *Cibicoides* spp.  $\delta^{18}\text{O}$  record of TN057-21 (Ninnemann et al., 1999) and the independently dated Atlantic benthic  $\delta^{18}\text{O}$  stack of Lisiecki and Raymo (2009), which provides support for our age model only within a multimillennial confidence range owing to the age uncertainties of the two records. However, our age model also agrees with the chronology of Barker and Diz (2014) within 500 years on average (Figure 4). This age model is based on an alignment of

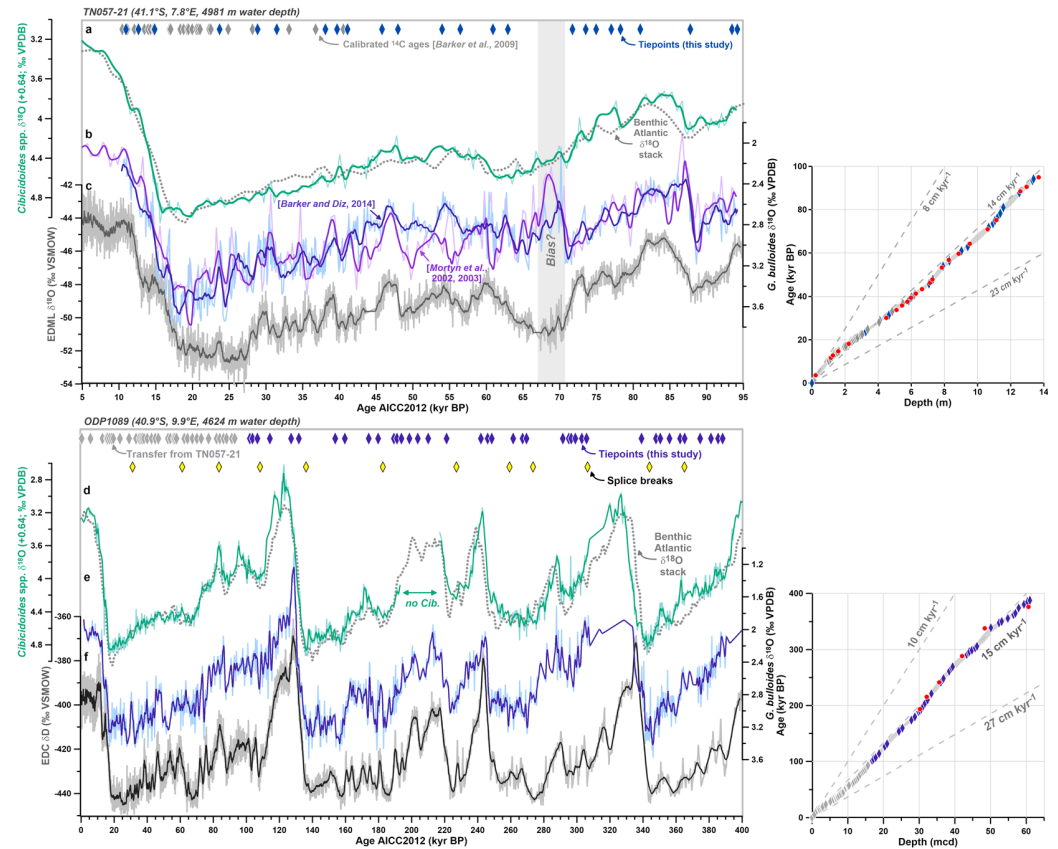


**Figure 4.** Age model (top) for sediment core TN057-21 and (bottom) for ODP Site 1089. (a) *Cibicidoides* spp.  $\delta^{18}\text{O}$  (green; Ninnemann et al., 1999) and the Atlantic benthic  $\delta^{18}\text{O}$  stack of Lisiecki and Raymo (2009; stippled), (b) *G. bulloides*  $\delta^{18}\text{O}$  data of Mortyn et al. (2002, 2003; purple) and Barker and Diz (2014; blue, depth scale adjusted), (c)  $\delta^{18}\text{O}$  of the Antarctic EPICA Dronning Maud Land (EDML) ice core (gray; EPICA Community Members, 2006), (d) *Cibicidoides* spp.  $\delta^{18}\text{O}$  (green; Hodell et al., 2001) and the Atlantic benthic  $\delta^{18}\text{O}$  stack of Lisiecki and Raymo (2009) (stippled), (e) *G. bulloides*  $\delta^{18}\text{O}$  (Mortyn et al., 2002, 2003), and (f) EPICA Dome C (EDC)  $\delta\text{D}$  (Jouzel et al., 2007). Symbols at the top of each panel indicate age markers (TN057-21:  $^{14}\text{C}$  dating [gray] and stratigraphic alignment of *G. bulloides*  $\delta^{18}\text{O}$  to Antarctic temperature variations [blue]; ODP Site 1089: tie points transferred from TN057-21 [gray] and from a stratigraphic alignment of *G. bulloides*  $\delta^{18}\text{O}$  and Antarctic temperature variations [blue], and splice breaks [yellow]). Insets on the right show age-depth relationships for the core sites in comparison to previous chronologies (red) for TN057-21 (Barker & Diz, 2014) and for ODP Site 1089 (Stoner et al., 2003), age uncertainties (gray envelopes) and sedimentation rates (stippled lines). Gray bar in the top panel indicates a potential bias of *G. bulloides*  $\delta^{18}\text{O}$  owing to seasonality or dissolution (Barker & Diz, 2014).

rapid increases in planktic foraminifer abundances and major Greenland stadial-interstadial transitions. However, to assess links to Northern Hemisphere climate records, we rely on the planktic  $\delta^{18}\text{O}$ -based age model to avoid circularity in reasoning. The TN057-21 age scale is transferred to the last glacial section of ODP Site 1089, by aligning the carbonate weight percentage records (supporting information Table S4).

A period of distinct mismatch between our *G. bulloides*  $\delta^{18}\text{O}$  record and EDML  $\delta^{18}\text{O}$  variations is MIS 4, between 70 and 65 kyr before present (BP; Figure 4). It has been proposed that intense dissolution and/or extreme seasonality of *G. bulloides* may account for this mismatch (Barker & Diz, 2014). The observed maximum in *Cibicidoides* spp.  $\delta^{18}\text{O}$  during MIS 4 supports the notion that the low planktic  $\delta^{18}\text{O}$  signal during MIS 4 is likely a temperature-independent artifact.

To obtain a chronology for ODP Site 1089 beyond the last glacial period, we have aligned *G. bulloides*  $\delta^{18}\text{O}$  variations with Antarctic temperature fluctuations represented by the  $\delta\text{D}$  record of the EPICA Dome C (EDC) ice core (Jouzel et al., 2007) that provides a continuous record for the last 400 kyr (Figure 4 and supporting information Table S4). This age model approach is broadly consistent with previous chronologies for ODP Site 1089 (Figure 4; Hodell et al., 2001, 2003; Stoner et al., 2003). Mean relative age uncertainties ( $2\sigma$ ) for ODP

Site 1089 estimated based on BChron are high ( $2,800 \pm 1,600$  years on average) owing to the large *G. bulloides*  $\delta^{18}\text{O}$  variability and an insufficient resolution of the data in parts of the record.

In addition, Charles et al. (2010) cautioned about undetected coring gaps at splice breaks of the composite sediment record at ODP Site 1089. Some of these splice breaks fall within intervals with little variation of the XRF Ca/Ti signal (e.g., Figure 4) and are therefore difficult to detect. A stratigraphic alignment of *G. bulloides*  $\delta^{18}\text{O}$  from ODP Site 1089 and the southwest Pacific sediment core MD97-2120 suggests that the time span of these gaps can be significant, for example, a few kiloyears (e.g., MIS 5/4 transition; Charles et al., 2010). However, this assessment assumes that both records are strictly synchronous and have experienced identical local hydrographic changes and effects from ice volume changes over time. Although the *Cibicides* spp.  $\delta^{18}\text{O}$  record of ODP Site 1089 is in good agreement with the Atlantic benthic  $\delta^{18}\text{O}$  stack of Lisiecki and Raymo (2009), supporting the overall stratigraphy, there is the possibility of gaps at splice breaks, which adds chronological uncertainties that may confound estimates of phase relationships, for instance, to Northern Hemisphere climate records.

## 4. Results

### 4.1. XRF Ca/Ti—An Indicator of the Carbonate Saturation State of the Deep Ocean

The XRF Ca/Ti ratio has been proposed to closely reflect changes in the proportions of terrestrial and calcareous material in marine sediments (Croudace & Rothwell, 2015). Titanium is exclusively of detrital origin and is nonreactive during early diagenetic processes (Bahr et al., 2005; Hodell et al., 2013), and sedimentary calcium is derived from calcareous remains of mostly planktic organisms. The logarithm of the XRF Ca/Ti ratio, denoted as log-XRF Ca/Ti ratio, has been proposed to reflect variations in the true elemental logarithmic ratios in the sediments (Weltje & Tjallingii, 2008). High correlation coefficients between changes in the log-XRF Ca/Ti ratio and the logarithm of carbonate weight percentages in our sediment cores (TN057-21:  $R^2 = 0.90$ , TN057-10:  $R^2 = 0.75$ , ODP Site 1089:  $R^2 = 0.90$ ; Figure 2) suggest that our XRF Ca/Ti data robustly represent a high-resolution record of carbonate content variations in our study cores.

The carbonate content of deep-sea sediments can be affected by dilution with noncarbonate material, such as biogenic silica (opal), changes in carbonate production in overlying surface water, and dissolution in the water column, in bottom waters and in pore waters. The dissolution control on carbonate is a complex signal that responds to both rapid transient changes in deep water hydrography and slow changes in the position of the lysocline and the CCD, as well as changes in local sedimentation rate and sediment porosity.

Fluxes of lithogenic and biogenic material such as alkenones and opal (indicators for export production of calcareous haptophyte algae and diatom frustules, respectively) to the deep sub-Antarctic Atlantic were shown to have gradually changed over millennial-scale climate events during the last glacial period in parallel with Antarctic dust fluxes (supporting information Figure S1; Anderson et al., 2014; Gottschalk et al., 2016; Martínez-García et al., 2014). This contrasts with rapid shifts in the  $\text{CaCO}_3$  content observed in TN057-21 and at ODP Site 1089 (Figure 5) and suggests that factors other than dilution and carbonate export production must have played a dominant role in changes in carbonate burial in the deep Cape Basin. Similarly, gradual dust-driven changes in carbon export to the deep Cape Basin as implied by the alkenone and opal flux records in the sub-Antarctic Atlantic (Anderson et al., 2014) may indicate that respiratory calcite dissolution has had a secondary influence on rapid variations in the carbonate content at our study sites. However, the flux of labile phytodetrital material to the deep Cape Basin was suggested to have increased during North Atlantic stadials despite low-productivity conditions (Diz & Barker, 2015), but it remains open to what extent these fluxes influenced the carbonate saturation in bottom water and pore water at our study sites. Our results show a close reciprocal correspondence between carbonate weight percentages and shell fragmentation (Figure 3), suggesting that both must result, to a large extent, from changes in partial sedimentary dissolution driven by variations in the carbonate saturation state of bottom water and/or pore water.

Sedimentation rates are high at our study sites (Figure 4), which favors carbonate preservation, although these sites are bathed in carbonate undersaturated water masses (supporting information Table S1). The high-sedimentation regime at our study sites therefore allows carbonates to be removed from the sediment mixed layer and buried in the sediment before being dissolved. This would in turn imply that changes in sediment focusing and in sedimentation rates related to the activity of bottom water currents may play a role in

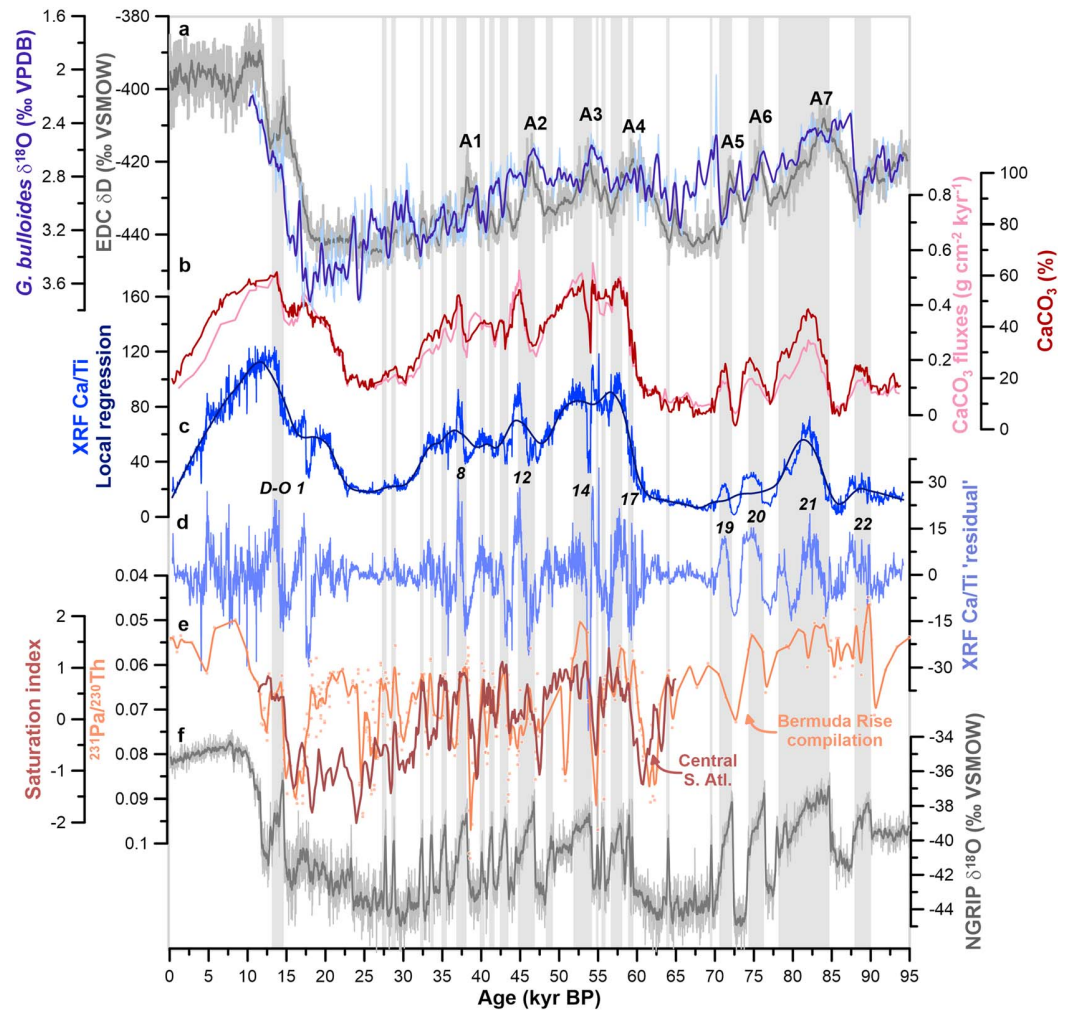


**Figure 5.** Low- and high-frequency components of the XRF Ca/Ti record of TN057-21. (a) EDC  $\delta D$  (gray; Jouzel et al., 2007) and *G. bulloides*  $\delta^{18}O$  (blue; Barker & Diz, 2014), (b) carbonate fluxes (purple) and carbonate weight percentages (red; Sachs & Anderson, 2003; Yu et al., 2014), (c) XRF Ca/Ti record (unfiltered, blue) and local weighted regression (LOESS, dark blue), (d) high-pass-filtered (suborbital) component of the XRF Ca/Ti record (residual), (e) saturation index in central South Atlantic core MD07-3076Q (dark brown) (Gottschalk et al., 2015) and the composite  $^{231}Pa/^{230}Th$  record from the Bermuda Rise after Henry et al. (2016; light brown), and (f) NGRIP  $\delta^{18}O$  (NGRIP members, 2004). All records are shown on the AICC2012 or equivalent GICC05 age scales (Veres et al., 2013). Dansgaard-Oeschger (D-O) and Antarctic warming events (A1–A7) are denoted according to Dansgaard et al. (1993) and Blunier and Brook (2001), respectively. Gray bars highlight NGRIP interstadials.

changing the carbonate preservation at our study sites. Because the reconstruction of sedimentation rates prior to the overprint from carbonate dissolution is difficult, we cannot entirely rule in or rule out the influence of this process on our proxy data or estimate its contribution with confidence. We therefore suggest that the XRF Ca/Ti ratios of our study cores serve as a high-resolution indicator of carbonate saturation changes in the deep Cape Basin consistent with previous propositions (Barker et al., 2010; Barker & Diz, 2014), although it is possible that the XRF Ca/Ti ratios were influenced by pore water dissolution effects and/or sedimentation rate changes.

#### 4.2. Carbonate Preservation Variability in the Sub-Antarctic Atlantic During the Last Glacial Cycle

Chronostratigraphy on millennial time scales is challenging, and correlating the time series of interest directly to either Antarctic or Greenland ice core records may introduce a circularity in reasoning. Charles et al. (1996) argued that the stratigraphic relationships observed among variables in sediment core RC11-83, a core in the

vicinity of TN057-21 (Figure 1), could be used to infer the relative phasing of different components of the ocean-climate system, thereby circumventing the chronological limitations associated with resolving millennial-scale climate events. They argued that the benthic  $\delta^{13}\text{C}$  shares many characteristics with the Greenland ice core temperature record, whereas planktic (*G. bulloides*)  $\delta^{18}\text{O}$  resembles Antarctic (ice core) temperature variations. The authors have further pointed out that planktic  $\delta^{18}\text{O}$  leads benthic  $\delta^{13}\text{C}$  and by extension suggests a phasing between Antarctic and Greenland warming that is consistent with the synchronization of methane records between Greenland and Antarctic ice cores (Blunier & Brook, 2001; EPICA Community Members, 2006). By examining stratigraphic relationships among planktic  $\delta^{18}\text{O}$  and partial sedimentary dissolution variables in TN057-21 in the depth domain, we arrive at a similar conclusion, despite some reservations that are discussed below.

Although the *G. bulloides*  $\delta^{18}\text{O}$  records of TN057-21 of Mortyn et al. (2002, 2003) and Barker and Diz (2014) show some differences, possibly due to intraspecific  $\delta^{18}\text{O}$  variability or differences in the number and size of foraminifera analyzed, *G. bulloides*  $\delta^{18}\text{O}$  minima in both records consistently precede or coincide with abrupt increases in carbonate weight percentages and XRF Ca/Ti ratios (Figure 3 and supporting information Figure S2). These increases also parallel marked peaks in planktic foraminifer abundances and decreases in foraminiferal fragmentation (Figure 3 and supporting information Figure S2), which suggests that *G. bulloides*  $\delta^{18}\text{O}$  minima are associated with major changes in sedimentary carbonate preservation in the deep Cape Basin, in a manner that appears to mimic the nature of Antarctic and Greenland (ice core) temperature changes.

Enhanced carbonate preservation parallels abrupt increases in benthic  $^{13}\text{C}$  and decreases in  $\epsilon_{\text{Nd}}$  in core TN057-21 that are indicative of an increased contribution of NADW to during these events (Figure 3; Charles et al., 1996; Piotrowski et al., 2008). The observed lead of  $\delta^{18}\text{O}$  minima over peaks in carbonate weight percentages and increases in the XRF Ca/Ti ratio in TN057-21 is supported by similar observations in TN057-10, where marked increases in *N. pachyderma*  $\delta^{18}\text{O}$  match or occur prior to rapid increases in the sedimentary carbonate content, shown by both enhanced carbonate weight percentages and elevated XRF Ca/Ti ratios (Figure 3). These combined observations suggest a close link of sedimentary carbonate preservation during or following peak Antarctic warming and a rapid incursion of NADW into the deep sub-Antarctic Atlantic during the last glacial period (Figure 3).

We find that marked transient carbonate preservation events coincide with strong and prolonged Greenland (i.e., Dansgaard-Oeschger, D-O) interstadials that follow major ice-rafting events in the North Atlantic ("Heinrich events"; e.g., Hemming, 2004; Figures 3 and 5). The two youngest carbonate peaks have been  $^{14}\text{C}$  dated to 14.2 and 37.5 kyr before present (BP) and correspond to Greenland (or D-O) interstadials 1 and 8, respectively (supporting information Table S3; Barker et al., 2009), the first representing the Bølling-Allerød warm period (Figures 3 and 5). Additional marked peaks in carbonate preservation are associated with D-O interstadials 14, 16, and 17 and with D-O interstadials 19 to 22 during late MIS 5 (Figures 3 and 5).

To accentuate the millennial-scale variability of our high-resolution XRF data, we removed the long-term trend by subtracting a local weighted regression (LOESS) with a bandwidth of 10 kyr. Large positive excursions in the high-frequency XRF Ca/Ti record are observed during those interstadials following Heinrich events, documenting major carbonate preservation events that are consistent with increased planktic foraminiferal abundances and decreased fragmentation (Figures 3 and 5). The high-pass-filtered XRF Ca/Ti signal also reveals weaker carbonate preservation events that generally coincide with shorter and weaker D-O interstadials not associated with Heinrich events (Figure 5). These smaller events coincide with preservation events in the central South Atlantic at shallower depth (core MD07-3076Q; Figure 5, location in Figure 1; Gottschalk et al., 2015).

Applying a high-pass filter to the XRF Ca/Ti data of ODP Site 1089, we observe coherence between the last glacial high-pass-filtered ("residual") XRF Ca/Ti variability of ODP Site 1089 and TN057-21 that broadly resembles North Atlantic climate variability during the last glacial period (Figure 6), although temporal offsets of  $740 \pm 400$  years ( $n = 11$ ) exist (Figure 6). These offsets can be (i) an artifact due to stratigraphic uncertainties (e.g., nature and millennial-scale accuracy of the stratigraphic alignment and coring gaps at splice breaks), (ii) a bias due to postburial processes such as bioturbation, or (iii) an accurate representation of the phasing. The first explanation strongly depends on the validity of the assumption that *G. bulloides*  $\delta^{18}\text{O}$  variations are in phase with Antarctic climate variability, which requires validation by independent proxies. Because the temporal offset is similar to the time lag between *G. bulloides*  $\delta^{18}\text{O}$  minima and the onset of enhanced

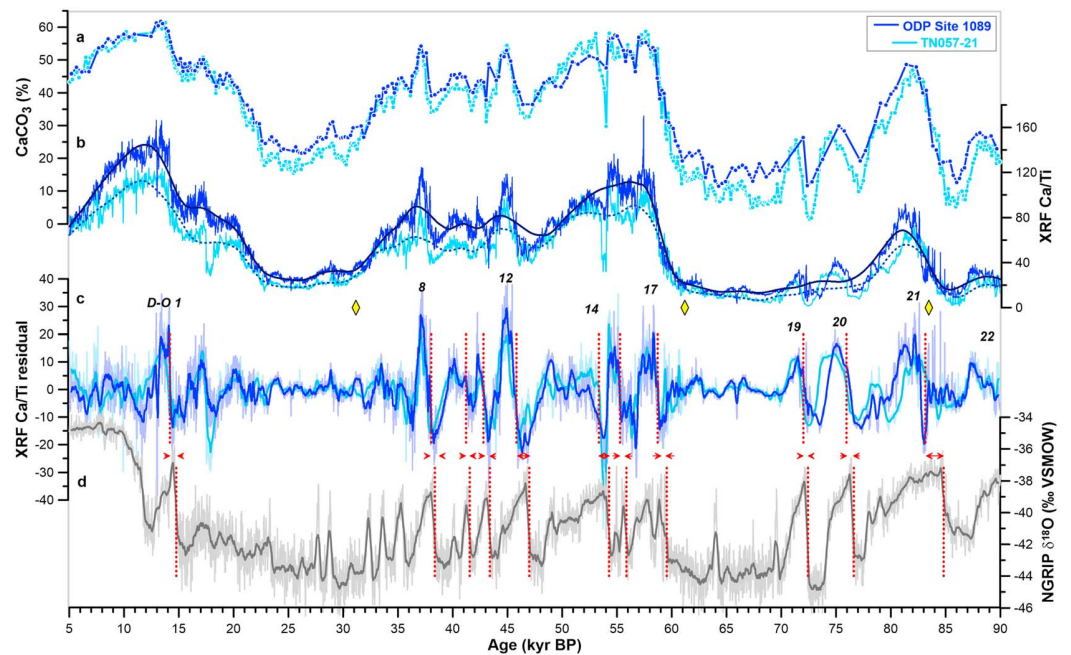


**Figure 6.** XRF Ca/Ti ratios of ODP Site 1089 (dark blue) and TN057-21 (light blue) during the last glacial period. (a) Carbonate weight percentages (Hodell et al., 2001, 2003; Sachs & Anderson, 2003); (b) XRF Ca/Ti ratios (unfiltered) and the associated LOESS fit (dark solid and stippled lines); yellow diamonds indicate splice breaks of ODP1089; (c) high-pass-filtered XRF Ca/Ti variability (residual), and (d) NGRIP  $\delta^{18}\text{O}$  (NGRIP members, 2004); red stippled lines indicate supposedly parallel events that are characterized by a mean temporal offset of  $740 \pm 400$  years ( $n = 11$ ); all records are shown on the AICC2012 or equivalent GICC05 age scales (Veres et al., 2013); D-O events are denoted according to Dansgaard et al. (1993).

carbonate burial in TN057-21 ( $1,030 \pm 690$  years,  $n = 11$ ; e.g., supporting information Figure S2), it is a direct consequence of the chosen age model approach and contrasts with the assumption of synchrony between carbonate preservation and Greenland interstadials made by Barker and Diz (2014). The second process (bioturbation effects) would act to reduce temporal offsets between *G. bulloides*  $\delta^{18}\text{O}$  minima and carbonate burial peaks, as shown by calculations with the simple sediment mixing model of Trauth (2013; supporting information Figure S3), and can therefore not explain our observations. The third explanation relies on the robustness of our chosen stratigraphy and may suggest that the transmission of Northern Hemisphere climate signals to the deep Cape Basin is delayed, which is discussed in detail below.

Deviations between the residual XRF Ca/Ti records of TN057-21 and ODP Site 1089, such as the strong negative anomaly in TN057-21 at 53.5 kyr BP, which is not present at ODP Site 1089 (Figure 6), may also originate from local effects, for instance, turbidites or burrows, although they seem overall less important for the observed carbonate variability. Nonetheless, the similarity and character of high-frequency XRF Ca/Ti variations at ODP Site 1089 and in core TN057-21 support the contention of fast and recurrent changes in the carbonate saturation state of the deep Cape Basin during the last glacial period for both long/strong and some short/weak North Atlantic climate events.

#### 4.3. Changes in Carbonate Preservation in the Sub-Antarctic Atlantic During the Last Four Glacial Cycles

Having demonstrated above that the XRF Ca/Ti variability is largely a reflection of varying carbonate dissolution and preservation (Figure 3) and that it is largely independent of local effects (Figure 6), we assess the XRF Ca/Ti variability observed at ODP Site 1089 to unravel the timing and nature of (sub)orbital-scale carbonate preservation changes beyond the last glacial cycle.

The low-frequency component of the XRF Ca/Ti data of ODP Site 1089 (i.e., the LOESS fit) indicates enhanced carbonate preservation during the early stages of interglacials and the late stages of glacial periods, whereas poor carbonate preservation prevailed during early glacial periods and interglacial-glacial transitions

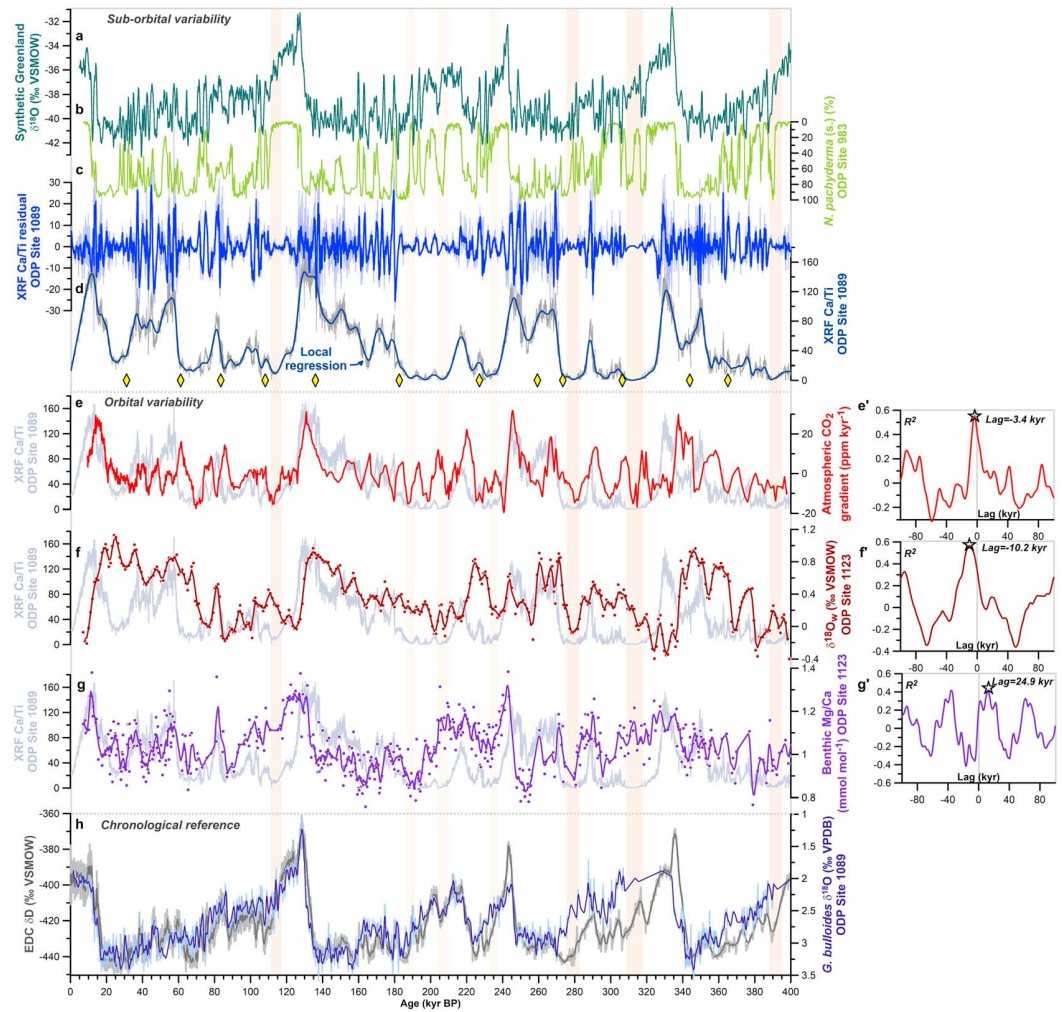


**Figure 7.** Low- and high-frequency components of the XRF Ca/Ti record of ODP Site 1089. (a) Synthetic Greenland  $\delta^{18}\text{O}$  record (Barker et al., 2011); (b) abundance changes of the cold-water species *N. pachyderma* at ODP Site 983 in the North Atlantic (Barker et al., 2015); (c) high-pass-filtered XRF Ca/Ti record (residual) of ODP Site 1089; (d) XRF Ca/Ti record of ODP Site 1089 (gray) and the associated LOESS fit (dark blue), replotted in light gray in (e) to (g); splice breaks of ODP Site 1089 are shown as yellow diamonds; (e) first derivative of the atmospheric  $\text{CO}_2$  record (red), which has maximum correlation with the XRF Ca/Ti record at lag =  $-3.4$  kyr (see correlation function in e'); (f) seawater  $\delta^{18}\text{O}$  ( $\delta^{18}\text{O}_w$ ) variations estimated at ODP Site 1123 (dark red; Elderfield et al., 2012), which has maximum correlation with the XRF Ca/Ti record at lag =  $-10.2$  kyr (see correlation function in f'); (g) *Uvigerina* spp. Mg/Ca record of ODP Site 1123, indicating bottom water temperature variations between  $-1.5^\circ\text{C}$  and  $3^\circ\text{C}$  (Elderfield et al., 2012) and showing maximum correlation with the XRF Ca/Ti record at lag =  $24.9$  kyr despite a high correlation coefficient at zero lag (see correlation function in g'); and (h) *G. bulloides*  $\delta^{18}\text{O}$  of ODP Site 1089 (blue; Mortyn et al., 2002, 2003) and EDC  $\delta\text{D}$  (gray) (Jouzel et al., 2007). All records are shown on the AICC2012 age scale. Vertical orange bars indicate quiet zones in carbonate burial, when carbonate contents approached zero.

(Figure 7). This is consistent with previous findings based on discrete carbonate measurements, which suggest a Pacific-like pattern of carbonate accumulation in the deep Cape Basin (Hodell et al., 2001, 2003). The suborbital (centennial- and millennial-scale) XRF Ca/Ti variability was particularly strong during glacial periods and terminations (Figure 7). Its amplitude over time is modulated by the overall sedimentary carbonate content, with higher carbonate content promoting higher-amplitude millennial-scale XRF Ca/Ti variations (Figure 7). In contrast, extended periods of low XRF Ca/Ti ratios with little residual variability occur when carbonate content is low/near zero, especially during glacial inceptions, that is, during the MIS 7/6 transition (Figure 8), and indicate prolonged periods of carbonate dissolution, causing the proxy to become saturated.

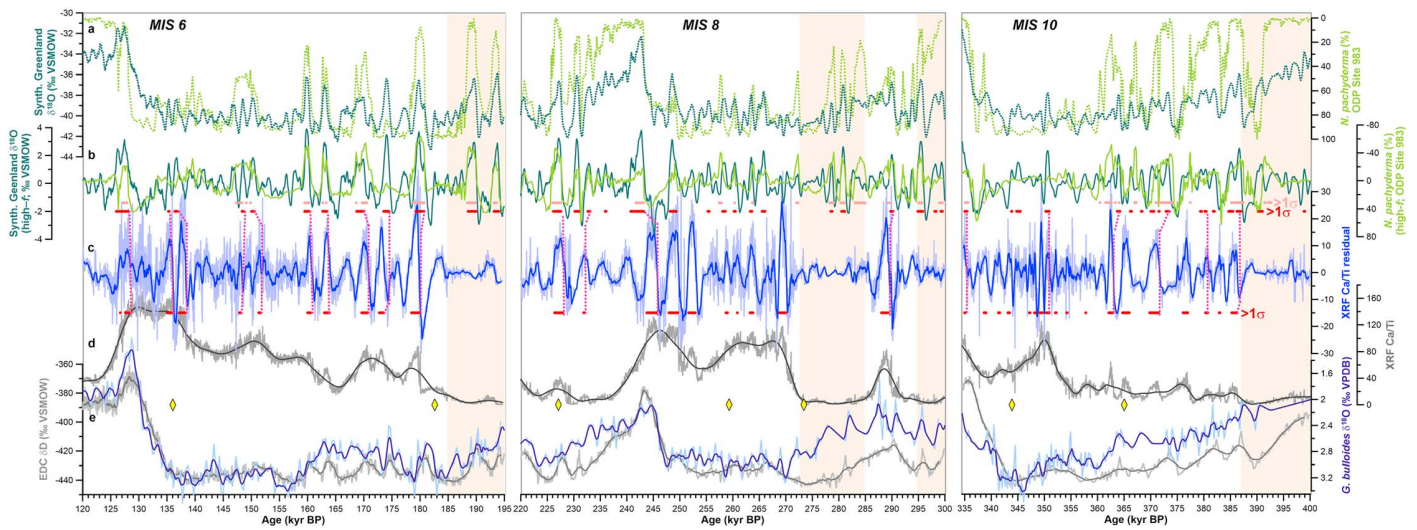


**Figure 8.** Low- and high-frequency components of the XRF Ca/Ti record of ODP Site 1089 during (left) MIS 6, (middle) MIS 8, and (right) MIS 10. (a) Abundance changes of the cold-water species *N. pachyderma* at ODP Site 983 in the North Atlantic (light green; Barker et al., 2015) and synthetic Greenland  $\delta^{18}\text{O}$  variations (dark green; Barker et al., 2011), (b) high-pass-filtered *N. pachyderma* abundance record at ODP Site 983 (i.e., variability after subtraction of a LOESS fit obtained with a 10 kyr bandwidth; light green; Barker et al., 2015) and synthetic high-frequency Greenland  $\delta^{18}\text{O}$  record (dark green; Barker et al., 2011), (c) high-pass-filtered XRF Ca/Ti record (residual) of ODP Site 1089, (d) XRF Ca/Ti record of ODP Site 1089 (gray) and the associated LOESS fit (black) with splice breaks shown as yellow diamonds, and (e) *G. bulloides*  $\delta^{18}\text{O}$  of ODP Site 1089 (blue; Barker & Diz, 2014) and EDC  $\delta\text{D}$  (gray; Jouzel et al., 2007). Horizontal red lines indicate the occurrence of interstadial conditions, that is, maxima in b and c that exceed a variability threshold of  $\sigma = 1$  (normalized; pale symbols refer to the record of ODP Site 983). Vertical stippled lines indicate presumably related events, while vertical orange bars indicate quiet zones in carbonate burial, when carbonate contents approached zero. All records are shown on the AICC2012 age scale.

Rapid changes towards higher XRF Ca/Ti ratios at ODP Site 1089 were often paralleled by increases in benthic  $\delta^{13}\text{C}$  (supporting information Figure S4)—a phenomenon that is also observed in core TN057-21. Except during “quiet zones” in carbonate burial, large-amplitude XRF Ca/Ti variations, for example, those exceeding one standard deviation, share features in the timing, grouping, and shape of Northern Hemisphere climate anomalies, as indicated by the synthetic Greenland  $\delta^{18}\text{O}$  record (Barker et al., 2011) or rapid *N. pachyderma* abundance changes at ODP Site 983 (Figure 8; Barker et al., 2015), despite millennial-scale temporal offsets. Phases of smaller-amplitude variability are broadly synchronous in both regions (e.g., 270–255 kyr BP and 155–140 kyr BP; Figure 8).

Most millennial-scale increases in the XRF Ca/Ti ratio and in benthic  $\delta^{13}\text{C}$  at ODP Site 1089 are preceded by *G. bulloides*  $\delta^{18}\text{O}$  minima (supporting information Figure S4), reminiscent of the stratigraphic links observed in TN057-21. However, it is difficult to unequivocally determine phase relationships, because the resolution of the planktic  $\delta^{18}\text{O}$  data at ODP Site 1089 is insufficient and the extent to which bioturbation has biased the signals is unconstrained (cf. supporting information Figure S3).

## 5. Discussion

### 5.1. Orbital Variability of Carbonate Preservation Changes in the South Atlantic

The bandwidth chosen for the LOESS fit of our XRF Ca/Ti data (10 kyr) is similar to the restoration time scale of carbonate compensation (~7–10 kyr; Anderson & Archer, 2002; Archer et al., 2000; Boyle, 1988b; Broecker & Peng, 1987). The low-frequency component of the XRF Ca/Ti data in the deep Cape Basin reflects glacial-interglacial variations in carbonate burial (Bickert & Wefer, 1996; Hodell et al., 2001) similar to those observed in the Indo-Pacific Ocean (Farrell & Prell, 1989; Howard & Prell, 1994; Peterson & Prell, 1985). As the signals are widespread in nature and occur across different productivity regimes (Anderson et al., 2008; Hodell et al., 2003), they are likely primarily driven by carbonate dissolution suggesting a common driver via carbonate compensation (Anderson et al., 2008; Hodell et al., 2001; Le & Shackleton, 1992) or other mechanisms (e.g., changes in global average respired carbon content).

Carbonate compensation may result from a range of different mechanisms, including variations in the (riverine) input of DIC and alkalinity to the ocean (Boyle, 1988a, 1988b; Broecker & Peng, 1987), changes in the deposition of carbonates on the continental shelf (Berger & Keir, 1984; Opdyke & Walker, 1992), adjustment of the ocean's (respired) nutrient inventories (Broecker, 1982; Broecker & Henderson, 1998; Falkowski, 1997), changes in the CaCO<sub>3</sub>-to-organic carbon export ratio (Archer et al., 2000; Archer & Maier-Reimer, 1994; Brzezinski et al., 2002), variations in the terrestrial carbon inventory (Broecker et al., 2001; Ridgwell et al., 2003), ocean circulation changes (Toggweiler, 1999), and combinations of these (e.g., polar alkalinity hypothesis; Broecker & Peng, 1989). It is not fully understood which of these trigger mechanisms has been the dominant influence on the ocean's carbonate system, how they have interacted over past glacial-interglacial cycles, if at all, and how this might have affected carbonate burial quantitatively (e.g., Archer et al., 2000; Berger & Keir, 1984; Broecker & Henderson, 1998; Opdyke & Walker, 1992; Ridgwell et al., 2003).

Based on cross-correlation analysis of  $\delta^{18}\text{O}$  SPECMAP stack and carbonate percentage changes in the deep Cape Basin, Hodell et al. (2001) suggested that ice volume changes, and hence sea level-driven shifts of (neritic versus pelagic) carbonate deposition, controlled deep ocean carbonate compensation in the Indo-Pacific and the deep Cape Basin (with a time lag of 7.6 kyr). However, benthic  $\delta^{18}\text{O}$  variations have long been known to be an imperfect representation of global ice volume changes owing to a significant temperature contribution (Elderfield et al., 2012; Labeyrie et al., 1987; Shackleton, 1967; Waelbroeck et al., 2002), especially on glacial/interglacial transitions (e.g., Skinner & Shackleton, 2005). Revisiting the analysis of Hodell et al. (2001) based on the temperature-corrected benthic seawater  $\delta^{18}\text{O}$  ( $\delta^{18}\text{O}_w$ ) record from ODP Site 1123 (Elderfield et al., 2012) while also taking advantage of the synchronized time scales between ODP Sites 1089 and 1123 (both are stratigraphically aligned to EDC), we find the highest correlation between carbonate deposition in the deep Cape Basin and fluctuations in global sea level over the last 400 kyr at a time lag of 10.2 kyr (Figure 7). As shown by a cross-correlation analysis with a 150-kyr moving window, this lag is time dependent and varies by 4.4 kyr (supporting information Figure S5). An identical lag (but with less variability over time,  $10.2 \pm 1.7$  kyr) is found through cross-correlation analysis of our deep Cape Basin CaCO<sub>3</sub> record and the global sea level record of Grant et al. (2014; supporting information Figure S5). These findings support the proposal of Hodell et al. (2001) that ice volume/sea level changes may be the trigger of deep ocean carbonate compensation.

However, other processes that are broadly synchronous with  $\delta^{18}\text{O}_w$  may also have triggered whole-ocean mass balance adjustments of the carbonate system or may have contributed to carbonate dissolution directly, for example, changes in the CaCO<sub>3</sub>-to-organic carbon ratio of exported detritus (Archer & Maier-Reimer, 1994), the waxing and waning of the terrestrial biosphere (Ridgwell et al., 2003), changes in the carbonate system dissociation constants owing to hydrostatic pressure, deep ocean temperature, and salinity variations (Kohfeld & Ridgwell, 2009; Ridgwell, 2001), changes in deep ocean carbon storage (Boyle, 1988b; Kerr et al., 2017) and ventilation (Tschumi et al., 2011), interbasin deep water and alkalinity exchange (Sosdian et al., 2018; Yu et al., 2014), or planetary outgassing of CO<sub>2</sub> (Broecker et al., 2015; Huybers & Langmuir, 2009). For instance, the good correspondence of bottom water temperatures at ODP Site 1123 and the low-frequency XRF Ca/Ti record (although maximum cross correlation is observed at lag = 24.9 kyr over the last 400 kyr; Figure 7) would suggest that some fraction of the orbital-scale carbonate variability may result from changes in hydrographic water mass properties, impacting on carbonate mineral solubility and ocean CO<sub>2</sub> solubility and possibly leading to carbonate compensation. Moreover, the water column density structure and vertical mixing in the Southern Ocean have varied over glacial-interglacial cycles (Hodell et al., 2003; Roberts et al., 2015), which may have modulated the whole-ocean mass balance response to perturbations of the ocean carbonate chemistry system or caused changes in carbonate preservation directly. Interestingly, it would appear that carbonate preservation changes in the deep Cape Basin are not dominated by major changes in volcanic CO<sub>2</sub> outgassing across glacial cycles (Broecker et al., 2015), as this would be expected to cause enhanced preservation during glacial inceptions and enhanced dissolution during deglaciations.

## 5.2. Suborbital Variability of Carbonate Preservation Changes in the South Atlantic

Previous findings have emphasized that strong carbonate preservation events in the deep Cape Basin primarily followed strong and long-lasting North Atlantic stadials and were driven by a recovery of North Atlantic overturning and concomitant increase in South Atlantic [CO<sub>3</sub><sup>2-</sup>] (Barker et al., 2010; Barker & Diz, 2014).

This is in line with distinct changes in the water mass indicator  $\epsilon_{\text{Nd}}$  and benthic foraminifer  $\delta^{13}\text{C}$  observed in sediment core TN057-21 (Ninnemann et al., 1999; Piotrowski et al., 2008; Figures 3 and 6), as well as variations in the mineralogy of detrital material at ODP Site 1089 (Kuhn & Diekmann, 2002). Some of the strong carbonate peaks were suggested to reflect NADW “overshoots,” when the export of NADW may have been greater than during the Holocene (Barker et al., 2010).

“Upstream” proxy evidence from the Gardar Drift in the North Atlantic manifest major increases in the formation of Iceland-Scotland Overflow Water (a major component of NADW) during strong and prolonged North Atlantic interstadials (i.e., D-O 8, 12, 14, and 16/17; Hodell et al., 2010), which is consistent with our observations. At the end of the last interglacial period, significant reorganizations of the deep western boundary current, a dominant pathway of NADW transport (Thornalley et al., 2013), are clearly reflected in carbonate weight percentages and XRF Ca/Ti ratios in the deep Cape Basin. These observations support the notion that major millennial-scale carbonate preservation events in the deep Cape Basin are controlled by a changing preponderance of NADW versus AABW and associated carbonate ion saturation changes at our core sites (Hodell et al., 2001).

The high-pass-filtered XRF Ca/Ti records of TN057-21 and at ODP Site 1089 suggest significant AMOC changes during subdued D-O cycles (Figure 6). Despite evidence for dynamical AMOC changes during D-O cycles (Kissel et al., 1999), clear benthic  $\delta^{13}\text{C}$  evidence for NADW changes during non-Heinrich D-O events in the North Atlantic remains sparse (Elliot et al., 2002; Keigwin & Boyle, 1999; Keigwin & Jones, 1994; Lynch-Stieglitz et al., 2014; Skinner et al., 2007). In contrast, Gottschalk et al. (2015) and Henry et al. (2016) provide evidence for changes in NADW export during nearly each North Atlantic D-O cycle of the last 60 kyr (Figure 5). Although the production and export rate of NADW may have been decoupled from the spatial extent of northern sourced water masses at times (McManus et al., 2004), the good agreement between rapid fluctuations in carbonate preservation in the deep Cape Basin and AMOC variability observed in the North Atlantic during MIS 3 (Figures 5 and 6) emphasizes the contention of fast changes in the southern extent of high- $[\text{CO}_3^{2-}]$  NADW during North Atlantic climate events.

It has been suggested that the rapid nature of changes in the southward extent of NADW and the position of the lysocline (i.e., the GNAIW/AABW boundary) during North Atlantic climate events were associated with the rapid propagation of oceanic waves, water mass end-member changes, and/or centennial-scale advective transport (Gottschalk et al., 2015). Transient changes in the position of the GNAIW/AABW boundary due to oceanic waves are likely more sensitively monitored at the shallower site of core MD07-3076Q (Gottschalk et al., 2015). The transmission of the same anomaly to the deeper Cape Basin may have required a stronger contribution from advection via CDW and vertical diffusion, and may have therefore been less efficient and slower. This may explain why long and strong D-O stadial-interstadial transitions are particularly pronounced in the sedimentary record of the deep Cape Basin, while events following non-Heinrich stadials are subdued and more weakly expressed. Due to the longer time scale required to influence the deepest ocean, this might also explain why carbonate preservation peaks in the deep Cape Basin significantly lag Greenland interstadials.

Millennial-scale variability in the high-pass-filtered XRF Ca/Ti ratios at ODP Site 1089 highlights the rapid nature of carbonate saturation changes during older glacial periods (Figures 7 and 8), which are broadly linked to abrupt climate variability in the Northern Hemisphere (Figure 8). The consistency between millennial-scale changes in the carbonate burial and North Atlantic climate variability, along with parallel changes in benthic  $\delta^{13}\text{C}$  at ODP Site 1089 for most events (supporting information Figure S4), indicates rapid changes in the extent of northern sourced water masses within the South Atlantic, and hence perturbations of the AMOC, analogous to what has been proposed for the last glacial period (Gottschalk et al., 2015). However, the amplitude of the high-frequency XRF Ca/Ti variability cannot be considered as reflection of the intensity of AMOC variations, because strong carbonate ion undersaturation during glacial inceptions, for instance, may dampen the sensitivity of the XRF Ca/Ti proxy, and a strong density stratification of the Southern Ocean water column during glacials may impede mixing between northern and southern sourced water masses (Roberts et al., 2015; Toggweiler, 1999), and hence a transmission of a North Atlantic climate signal to the deep Cape Basin. Irrespective of these factors masking the amplitude of the recorded events, we conclude that recurrent AMOC changes were dominant features of (de)glacial periods of the last 400 kyr that were rapidly communicated to the southern high latitudes but whose exact timing with respect to North Atlantic climate events (within centuries) remains to be confirmed.

### 5.3. Implications for Changes in Atmospheric CO<sub>2</sub>

Restoration of the ocean's alkalinity balance due to changes in the ocean's average alkalinity can lead to changes in the partitioning of CO<sub>2</sub> between the ocean and the atmosphere (Broecker, 1982; Broecker & Peng, 1987). Changes in the position of the lysocline and the CCD in the ocean as seen in orbital-scale changes of the XRF Ca/Ti record of ODP Site 1089 are a manifestation of these mass balance adjustments without directly revealing the mechanisms that might have controlled them. Model simulations remain inconclusive regarding the magnitude of atmospheric CO<sub>2</sub> change that would have resulted from glacial-interglacial variations in the position of the lysocline (Hain et al., 2010; Heinze et al., 1991; Sigman et al., 1998). We have emphasized a possible sea level control of carbonate compensation primarily in the Indo-Pacific Ocean that is qualitatively consistent with a varying output of alkalinity from the deep ocean due to variations in neritic carbonate deposition (Berger & Keir, 1984; Opdyke & Walker, 1992), but at the same time this does not rule out other drivers (Archer & Maier-Reimer, 1994; Boyle, 1988b; Broecker, 1982). Indeed, there is support for a longer-term (glacial-interglacial) contribution from varying respired carbon retention/release from the deep ocean, contributing to carbonate dissolution in the deep ocean during periods of CO<sub>2</sub> drop and carbonate preservation during CO<sub>2</sub> rise (Boyle, 1988a; de la Fuente et al., 2017; Kerr et al., 2017; Tschumi et al., 2011). Overall, the close agreement between changes in the carbonate burial in the deep Cape Basin and the *rate* of atmospheric CO<sub>2</sub> change within a few millennia (Figure 7) underlines the potential influence of marine carbonate chemistry (as modulated by ocean circulation and/or sea level change) on atmospheric CO<sub>2</sub>.

Fast dynamical, physical, and biological processes involving adjustments of the AMOC and the atmospheric circulation were associated with millennial changes in atmospheric CO<sub>2</sub> (Anderson et al., 2009; Gottschalk et al., 2016; Jaccard et al., 2016; Martínez-García et al., 2014; Skinner et al., 2010, 2014). Some model simulations that force a slowdown of the AMOC (e.g., through freshwater hosing) have shown an increase in atmospheric CO<sub>2</sub> as a result of oceanic carbon release, primarily in the southern high latitudes (e.g., Schmittner & Galbraith, 2008), which is consistent with our inference of suppressed NADW export at times of rising atmospheric CO<sub>2</sub>.

We surmise an additional mechanism through which variations in NADW export to the southern high latitudes may have influenced the sequestration of respired carbon in the deep Southern Ocean, primarily through the carbonate system. Epibenthic foraminiferal B/Ca ratios measured on glacial sediments from the Atlantic indicate an ~20–30 μmol/kg increase of GNAIW [CO<sub>3</sub><sup>2-</sup>] at 1–2 km and a decrease by ~20 μmol/kg at sites deeper than ~3.5 km (Gottschalk et al., 2015; Lacerra et al., 2017; Sosdian et al., 2018; Yu et al., 2008, 2010, 2016; Yu, Anderson, et al., 2013), while North Atlantic surface water [CO<sub>3</sub><sup>2-</sup>] was elevated by 60 μmol/kg relative to the late Holocene (Yu, Thornalley, et al., 2013). This was likely due to air-sea gas equilibration at lower atmospheric CO<sub>2</sub> concentrations (Barker & Elderfield, 2002; Hönisch & Hemming, 2005) and supports the contention that GNAIW had significantly higher preformed [CO<sub>3</sub><sup>2-</sup>] values. The increased contribution of northern sourced water masses with higher preformed [CO<sub>3</sub><sup>2-</sup>] to the deep Atlantic and the Southern Oceans during interstadials may have played a role in titrating respiratory CO<sub>2</sub> that had accumulated in the deep Atlantic and the Southern Ocean through the ocean soft-tissue pump. This would have increased the buffer capacity (i.e., Revelle factor) of water being upwelled in the southern high latitudes, essentially reducing aqueous [CO<sub>2</sub>] (and therefore *p*CO<sub>2</sub> for a given DIC), provided that the density stratification of the water column allowed sufficient mixing of northern sourced water masses into upwelling CDW. If these water masses made contact with the air-sea interface, it would have slowed CO<sub>2</sub> degassing from upwelled water to the atmosphere. This titration effect may have therefore contributed to a decline of atmospheric CO<sub>2</sub> during millennial-scale climate events during mild glacial conditions, for example, during the long and strong South Atlantic carbonate preservation peaks. Although the impact of this titration effect on millennial-scale atmospheric CO<sub>2</sub> variations, in particular during prolonged/strong versus short/weak D-O cycles, needs to be assessed quantitatively, it may provide a secondary mechanism for interhemispheric coupling and changes in atmospheric CO<sub>2</sub> on millennial time scales.

## 6. Conclusions

We reconstruct and analyze carbonate weight percentage changes of the last four glacial cycles in three sediment cores from the deep Cape Basin (Southeast Atlantic; TN057-21, TN057-10, and ODP Site 1089)

based on high-resolution XRF Ca/Ti records. The XRF Ca/Ti data are consistent with discrete carbonate measurements. Based on auxiliary data, we argue that past variations in carbonate burial in the Cape Basin reflect variations in the carbonate saturation (i.e., the corrosiveness) of local bottom water and/or pore water.

We suggest that the low-frequency (“orbital-scale”) XRF Ca/Ti variability reflects carbonate compensation and changes in deep ocean respired carbon storage. The high-frequency (suborbital-scale) XRF Ca/Ti component largely reflects the redistribution of carbonate ions through changes in deep water circulation. We find that carbonate preservation peaks are generally linked with Northern Hemisphere D-O interstadials during the last glacial cycle, despite differences in amplitude and in submillennial timing that may have both sedimentary (e.g., age model uncertainties) and hydrographic causes (e.g., transmission timescale of climate signals through the Atlantic). We suggest that these events are linked with recurrent perturbations of the AMOC, which is consistent with proxy data from the central South Atlantic (Gottschalk et al., 2015) and from upstream sites in the North Atlantic (Henry et al., 2016; Kissel et al., 1999; Lynch-Stieglitz et al., 2014; Margari et al., 2010; Skinner et al., 2007).

Although age uncertainties are high, and event amplitudes may be masked by secondary processes, the high-pass-filtered XRF Ca/Ti variability at ODP Site 1089 indicates that older glacial periods were characterized by similar carbonate preservation events, whose timing and structure share similarities with the “synthetic Greenland record” of Barker et al. (2011) and North Atlantic surface ocean variability (Barker et al., 2015). This would indicate frequent AMOC perturbations and their rapid transmission throughout the Atlantic basin during older glacial periods, offering further validation of the underlying hypotheses of Greenland climate predictions on the basis of Antarctic ice cores and the “bipolar seesaw” (Barker et al., 2011).

We suggest that our XRF data indicate distinct rapid and recurrent AMOC variability during the past four glacial periods, which may have had a direct impact on changes in atmospheric CO<sub>2</sub> through a “titration effect.” Newly formed glacial NADW with a higher preformed [CO<sub>3</sub><sup>2-</sup>] signature and transmitted rapidly to the Southern Ocean may have slowed down CO<sub>2</sub> outgassing in the southern high latitudes, especially during Northern Hemisphere interstadials, through shifts in the aqueous carbonate speciation of upwelling waters away from CO<sub>2</sub> (i.e., by increasing the buffering capacity of the deep South Atlantic and Southern Ocean). The resulting impact of AMOC changes on atmospheric CO<sub>2</sub> levels during D-O cycles remains, however, to be quantified.

#### Acknowledgments

J. G. acknowledges support from the Swiss National Science Foundation (grant 200021\_163003), the German Research Foundation (grant GO 2294/2-1), and the Gates Cambridge Trust. D.A.H. thanks the European Research Council (WIHM#339694) for support. L. C. S. acknowledges the Royal Society, the Cambridge Isaac Newton Trust, and NERC grant NE/J010545/1. S. L. J. was funded by the Swiss National Science Foundation (grants PP00P2-144811 and PP002\_172915). We thank Maryline Vautravers (Godwin Laboratory for Palaeoclimate Research, University of Cambridge) for performing and providing high-resolution sedimentary census counts from core TN057-21 and Bob Anderson (Lamont-Doherty Earth Observatory, Columbia University) for providing U and Th radioisotope data of TN057-21 from previous publications. We are grateful to Jimin Yu, Min-Te Chen, and one anonymous reviewer for their constructive feedback on this study. Data presented in this study are available from PANGAEA (<https://doi.org/10.1594/PANGAEA.887160>).

#### References

- Anderson, D. M., & Archer, D. (2002). Glacial-interglacial stability of ocean pH inferred from foraminifer dissolution rates. *Nature*, *416*(6876), 70–73. <https://doi.org/10.1038/416070a>
- Anderson, R. F., Ali, S., Bradtmiller, L. I., Nielsen, S. H. H., Fleisher, M. Q., Anderson, B. E., & Burckle, L. H. (2009). Wind-driven upwelling in the Southern Ocean and the deglacial rise in atmospheric CO<sub>2</sub>. *Science*, *323*(5920), 1443–1448. <https://doi.org/10.1126/science.1167441>
- Anderson, R. F., Barker, S., Fleisher, M., Gersonde, R., Goldstein, S. L., Kuhn, G., et al. (2014). Biological response to millennial variability of dust and nutrient supply in the Subantarctic South Atlantic Ocean. *Philosophical Transactions of the Royal Society*, *372*(2019), 20130054. <https://doi.org/10.1098/rsta.2013.0054>
- Anderson, R. F., Fleisher, M. Q., Lao, Y., & Winckler, G. (2008). Modern CaCO<sub>3</sub> preservation in equatorial Pacific sediments in the context of late-Pleistocene glacial cycles. *Marine Chemistry*, *111*(1–2), 30–46. <https://doi.org/10.1016/j.marchem.2007.11.011>
- Antonov, J. I., Seidov, D., Boyer, T. P., Locarnini, R. A., Mishonov, A. V., Garcia, H. E., et al. (2010). In S. Levitus (Ed.), *World Ocean Atlas 2009, Vol. 2: Salinity*, NOAA Atlas NESDIS (Vol. 69, p. 184). Washington, DC: U.S. Government Printing Office.
- Archer, D., & Maier-Reimer, E. (1994). Effect of deep-sea sedimentary calcite preservation on atmospheric CO<sub>2</sub> concentration. *Nature*, *367*(6460), 260–263. <https://doi.org/10.1038/367260a0>
- Archer, D., Winguth, A., Lea, D., & Mahowald, N. (2000). What caused the glacial/interglacial atmospheric pCO<sub>2</sub> cycles? *Reviews of Geophysics*, *38*(2), 159–189. <https://doi.org/10.1029/1999RG000066>
- Archer, D. E. (1996). An atlas of the distribution of calcium carbonate in sediments of the deep sea. *Global Biogeochemical Cycles*, *10*(1), 159–174. <https://doi.org/10.1029/95GB03016>
- Bahr, A., Lamy, F., Arz, H., Kuhlmann, H., & Wefer, G. (2005). Late glacial to Holocene climate and sedimentation history in the NW Black Sea. *Marine Geology*, *214*(4), 309–322. <https://doi.org/10.1016/j.margeo.2004.11.013>
- Balsam, W. L., & McCoy, F. W. (1987). Atlantic sediments: Glacial/interglacial comparisons. *Paleoceanography*, *2*(5), 531–542. <https://doi.org/10.1029/PA002i005p0531>
- Barker, S., Chen, J., Gong, X., Jonkers, L., Knorr, G., & Thornalley, D. (2015). Icebergs not the trigger for North Atlantic cold events. *Nature*, *520*(7547), 333–336. <https://doi.org/10.1038/nature14330>
- Barker, S., & Diz, P. (2014). Timing of the descent into the last ice age determined by the bipolar seesaw. *Paleoceanography*, *29*, 489–507. <https://doi.org/10.1002/2014PA002623>
- Barker, S., Diz, P., Vautravers, M. J., Pike, J., Knorr, G., Hall, I. R., & Broecker, W. S. (2009). Interhemispheric Atlantic seesaw response during the last deglaciation. *Nature*, *457*(7233), 1097–1102. <https://doi.org/10.1038/nature07770>

- Barker, S., & Elderfield, H. (2002). Foraminiferal calcification response to glacial-interglacial changes in atmospheric CO<sub>2</sub>. *Science*, 297(5582), 833–836. <https://doi.org/10.1126/science.1072815>
- Barker, S., Knorr, G., Edwards, R. L., Parrenin, F., Putnam, A. E., Skinner, L. C., et al. (2011). 800,000 years of abrupt climate variability. *Science*, 334(6054), 347–351. <https://doi.org/10.1126/science.1203580>
- Barker, S., Knorr, G., Vautravers, M. J., Diz, P., & Skinner, L. C. (2010). Extreme deepening of the Atlantic overturning circulation during deglaciation. *Nature Geoscience*, 3(8), 567–571. <https://doi.org/10.1038/ngeo921>
- Bazin, L., Landais, A., Lemieux-Dudon, B., Toyé Mahamadou Kele, H., Veres, D., Parrenin, F., et al. (2013). An optimized multi-proxy, multi-site Antarctic ice and gas orbital chronology (AICC2012): 120–800 ka. *Climate of the Past*, 9(4), 1715–1731. <https://doi.org/10.5194/cp-9-1715-2013>
- Berger, W. H., & Keir, R. S. (1984). Glacial-Holocene changes in atmospheric CO<sub>2</sub> and the deep-sea record. In J. E. Hansen, & T. Takahashi (Eds.), *Climate processes and climate sensitivity, Geophysical Monograph Series* (Vol. 29, pp. 337–351). Washington DC: American Geophysical Union.
- Bickert, T., & Wefer, G. (1996). Late Quaternary deep water circulation in the South Atlantic: Reconstruction from carbonate dissolution and benthic stable isotopes. In G. Wefer, W. H. Berger, G. Siedler, & D. J. Webb (Eds.), *The South Atlantic: Present and past circulation* (pp. 599–620). Berlin-Heidelberg: Springer. [https://doi.org/10.1007/978-3-642-80353-6\\_30](https://doi.org/10.1007/978-3-642-80353-6_30)
- Biscaye, P. E., Kolla, V., & Turekian, K. K. (1977). Distribution of calcium carbonate in surface sediments of the Atlantic Ocean. *Journal of Geophysical Research*, 82(6), 997–998. <https://doi.org/10.1029/JC082i006p00997>
- Blunier, T., & Brook, E. J. (2001). Timing of millennial-scale climate change in Antarctica and Greenland during the last glacial period. *Science*, 291(5501), 109–112. <https://doi.org/10.1126/science.291.5501.109>
- Bouttes, N., Roche, D. M., & Paillard, D. (2012). Systematic study of the impact of fresh water fluxes on the glacial carbon cycle. *Climate of the Past*, 8(2), 589–607. <https://doi.org/10.5194/cp-8-589-2012>
- Boyle, E. A. (1988a). The role of vertical chemical fractionation in controlling late Quaternary atmospheric carbon dioxide. *Journal of Geophysical Research*, 93(C12), 15,701–15,714. <https://doi.org/10.1029/JC093iC12p15701>
- Boyle, E. A. (1988b). Vertical oceanic nutrient fractionation and glacial/interglacial CO<sub>2</sub> cycles. *Nature*, 331(6151), 55–56. <https://doi.org/10.1038/331055a0>
- Broecker, W. (1982). Glacial to interglacial changes in ocean chemistry. *Progress in Oceanography*, 11(2), 151–197. [https://doi.org/10.1016/0079-6611\(82\)90007-6](https://doi.org/10.1016/0079-6611(82)90007-6)
- Broecker, W. S., & Clark, E. (2001). Glacial-to-Holocene redistribution of carbonate ion in the deep sea. *Science*, 294(5549), 2152–2155. <https://doi.org/10.1126/science.1064171>
- Broecker, W. S., & Henderson, G. M. (1998). The sequence of events surrounding Termination II and their implications for the cause of glacial-interglacial CO<sub>2</sub> changes. *Paleoceanography*, 13(4), 352–364. <https://doi.org/10.1029/98PA00920>
- Broecker, W. S., Lynch-Stieglitz, J., Clark, E., Hajdas, I., & Bonani, G. (2001). What caused the atmosphere's CO<sub>2</sub> content to rise during the last 8000 years? *Geochemistry, Geophysics, Geosystems*, 2(10), 1062–1073. <https://doi.org/10.1029/2001GC000177>
- Broecker, W. S., & Peng, T. H. (1987). The role of CaCO<sub>3</sub> compensation in the glacial to interglacial atmospheric CO<sub>2</sub> change. *Global Biogeochemical Cycles*, 1(1), 15–29. <https://doi.org/10.1029/GB001i001p00015>
- Broecker, W. S., & Peng, T.-H. (1989). The cause of the glacial to interglacial atmospheric CO<sub>2</sub> change: A polar alkalinity hypothesis. *Global Biogeochemical Cycles*, 3(3), 215–239. <https://doi.org/10.1029/GB003i003p00215>
- Broecker, W. S., Yu, J., & Putnam, A. E. (2015). Two contributors to the glacial CO<sub>2</sub> decline. *Earth and Planetary Science Letters*, 429, 191–196. <https://doi.org/10.1016/j.epsl.2015.07.019>
- Brzezinski, M. A., Pride, C. J., Franck, V. M., Sigman, D. M., Sarmiento, J. L., Matsumoto, K., et al. (2002). A switch from Si(OH)<sub>4</sub> to NO<sub>3</sub><sup>-</sup> depletion in the glacial Southern Ocean. *Geophysical Research Letters*, 29(12), 1564. <https://doi.org/10.1029/2001GL014349>
- Channell, J. E. T., Stoner, J. S., Hodell, D. A., & Charles, C. D. (2000). Geomagnetic paleointensity for the last 100 kyr from the sub-Antarctic South Atlantic: A tool for inter-hemispheric correlation. *Earth and Planetary Science Letters*, 175(1–2), 145–160. [https://doi.org/10.1016/S0012-821X\(99\)00285-X](https://doi.org/10.1016/S0012-821X(99)00285-X)
- Charles, C. D., Lynch-Stieglitz, J., Ninnemann, U. S., & Fairbanks, R. G. (1996). Climate connections between the hemisphere revealed by deep sea sediment core/ice core correlations. *Earth and Planetary Science Letters*, 142(1–2), 19–27. [https://doi.org/10.1016/0012-821X\(96\)00083-0](https://doi.org/10.1016/0012-821X(96)00083-0)
- Charles, C. D., Pahnke, K., Zahn, R., Mortyn, P. G., Ninnemann, U., & Hodell, D. A. (2010). Millennial scale evolution of the Southern Ocean chemical divide. *Quaternary Science Reviews*, 29(3–4), 399–409. <https://doi.org/10.1016/j.quascirev.2009.09.021>
- Croudace, I. W., & Rothwell, R. G. (2015). *Micro-XRF studies of sediment cores: Applications of a non-destructive tool for the environmental sciences, Developments in Paleoenvironmental Research* (Vol. 17, p. 656). Dordrecht Heidelberg New York London: Springer. <https://doi.org/10.1007/978-94-017-9849-5>
- Crowley, T. J. (1985). Late Quaternary carbonate changes in the North Atlantic and Atlantic/Pacific comparisons. In E. T. Sundquist, & W. S. Broecker (Eds.), *The carbon cycle and atmospheric CO<sub>2</sub>: Natural variations Archaean to present* (pp. 271–284). Washington, DC: American Geophysical Union. <https://doi.org/10.1029/GM032p0271>
- Dansgaard, W., Johnsen, S. J., Clausen, H. B., Dahl-Jensen, D., Gundestrup, N. S., Hammer, C. U., et al. (1993). Evidence for general instability of past climate from a 250-kyr ice-core record. *Nature*, 364(6434), 218–220. <https://doi.org/10.1038/364218a0>
- de la Fuente, M., Calvo, E., Skinner, L. C., Pelejero, C., Evans, D., Müller, W., et al. (2017). The evolution of deep ocean chemistry and respired carbon in the eastern equatorial Pacific over the last deglaciation. *Paleoceanography*, 32, 1371–1385. <https://doi.org/10.1002/2017PA003155>
- Diz, P., & Barker, S. (2015). Linkages between rapid climate variability and deep-sea benthic foraminifera in the deep Subantarctic South Atlantic during the last 95 kyr. *Paleoceanography*, 30, 601–611. <https://doi.org/10.1002/2015PA002784>
- Elderfield, H., Ferretti, P., Greaves, M., Crowhurst, S., McCave, I. N., Hodell, D., & Piotrowski, A. M. (2012). Evolution of ocean temperature and ice volume through the Mid-Pleistocene climate transition. *Science*, 337(6095), 704–709. <https://doi.org/10.1126/science.1221294>
- Elliot, M., Labeyrie, L., & Duplessy, J.-C. (2002). Changes in North Atlantic deep-water formation associated with the Dansgaard-Oeschger temperature oscillations (60–10 ka). *Quaternary Science Reviews*, 21(10), 1153–1165. [https://doi.org/10.1016/S0277-3791\(01\)00137-8](https://doi.org/10.1016/S0277-3791(01)00137-8)
- Engleman, E. E., Jackson, L. L., & Norton, D. R. (1985). Determination of carbonate carbon in geological materials by coulometric titration. *Chemical Geology*, 53(1–2), 125–128. [https://doi.org/10.1016/0009-2541\(85\)90025-7](https://doi.org/10.1016/0009-2541(85)90025-7)
- EPICA Community Members (2006). One-to-one coupling of glacial climate variability in Greenland and Antarctica. *Nature*, 444(7116), 195–198. <https://doi.org/10.1038/nature05301>
- Falkowski, P. G. (1997). Evolution of the nitrogen cycle and its influence on the biological sequestration of CO<sub>2</sub> in the ocean. *Nature*, 387(6630), 272–275. <https://doi.org/10.1038/387272a0>
- Farrell, J. W., & Prell, W. L. (1989). Climatic change and CaCO<sub>3</sub> preservation: An 800,000 year bathymetric reconstruction from the central equatorial Pacific Ocean. *Paleoceanography*, 4(4), 447–466. <https://doi.org/10.1029/PA004i004p00447>

- Gottschalk, J., Skinner, L. C., Lippold, J., Vogel, H., Frank, N., Jaccard, S. L., & Waelbroeck, C. (2016). Biological and physical controls in the Southern Ocean on past millennial-scale atmospheric CO<sub>2</sub> changes. *Nature Communications*, 7, 11539. <https://doi.org/10.1038/ncomms11539>
- Gottschalk, J., Skinner, L. C., Misra, S., Waelbroeck, C., Menviel, L., & Timmermann, A. (2015). Abrupt changes in the southern extent of North Atlantic Deep Water during Dansgaard-Oeschger events. *Nature Geoscience*, 8(12), 950–954. <https://doi.org/10.1038/ngeo2558>
- Grant, K. M., Rohling, E. J., Bar-Matthews, M., Ayalon, A., Medina-Elizalde, M., Ramsey, C. B., et al. (2012). Rapid coupling between ice volume and polar temperature over the past 50,000 years. *Nature*, 491(7426), 744–747. <https://doi.org/10.1038/nature11593>
- Grant, K. M., Rohling, E. J., Ramsey, C. B., Cheng, H., Edwards, R. L., Florindo, F., et al. (2014). Sea-level variability over five glacial cycles. *Nature Communications*, 5(1), 1–9. <https://doi.org/10.1038/ncomms6076>
- Haddad, G. A., & Droxler, A. W. (1996). Metastable CaCO<sub>3</sub> dissolution at intermediate water depths of the Caribbean and western North Atlantic: implications for intermediate water circulation during the past 200,000 years. *Paleoceanography*, 11(6), 701–716. <https://doi.org/10.1029/96PA02406>
- Hain, M. P., Sigman, D. M., & Haug, G. H. (2010). Carbon dioxide effects of Antarctic stratification, North Atlantic Intermediate Water formation, and subantarctic nutrient drawdown during the last ice age: Diagnosis and synthesis in a geochemical box model. *Global Biogeochemical Cycles*, 24, GB4023. <https://doi.org/10.1029/2010GB003790>
- Haslett, J., & Parnell, A. (2008). A simple monotone process with application to radiocarbon-dated depth chronologies. *Journal of the Royal Statistical Society*, 57(4), 399–418. <https://doi.org/10.1111/j.1467-9876.2008.00623.x>
- Heinze, C., Maier-Reimer, E., & Winn, K. (1991). Glacial pCO<sub>2</sub> reduction by the world ocean: Experiments with the Hamburg carbon cycle model. *Paleoceanography*, 6(4), 395–430. <https://doi.org/10.1029/91PA00489>
- Hemming, S. R. (2004). Heinrich events: Massive late Pleistocene detritus layers of the North Atlantic and their global climate imprint. *Reviews of Geophysics*, 42, RG1005. <https://doi.org/10.1029/2003RG000128>
- Henrich, R., Baumann, K.-H., Gerhardt, S., Gröger, M., & Volbers, A. (2003). Carbonate preservation in deep and intermediate water masses in the South Atlantic: Evaluation and geological record (a review). In G. Wefer, S. Mulitza, & V. Ratmeyer (Eds.), *The South Atlantic in the Late Quaternary: Reconstruction of Material Budgets and Current Systems* (pp. 645–670). Berlin Heidelberg New York Tokyo: Springer. [https://doi.org/10.1007/978-3-642-18917-3\\_28](https://doi.org/10.1007/978-3-642-18917-3_28)
- Henry, L. G., McManus, J. F., Curry, W. B., Roberts, N. L., Piotrowski, A. M., & Keigwin, L. D. (2016). North Atlantic Ocean circulation and abrupt climate change during the last glaciation. *Science*, 353(6298), 470–474. <https://doi.org/10.1126/science.aaf5529>
- Hodell, D., Crowhurst, S., Skinner, L., Tzedakis, P. C., Margari, V., Channell, J. E. T., et al. (2013). Response of Iberian Margin sediments to orbital and suborbital forcing over the past 420 ka. *Paleoceanography*, 28, 185–199. <https://doi.org/10.1002/palo.20017>
- Hodell, D. A., Charles, C. D., Curtis, J. H., Mortyn, P. G., Ninnemann, U. S., & Venz, K. A. (2003). Data report: Oxygen isotope stratigraphy of ODP Leg 177 Sites 1088, 1089, 1090, 1093, and 1094. In *Proceedings of the Ocean Drilling Program, Scientific Results* (Vol. 177, pp. 1–26). College Station, TX: Ocean Drilling Program.
- Hodell, D. A., Charles, C. D., & Ninnemann, U. S. (2000). Comparison of interglacial stages in the South Atlantic sector of the southern ocean for the past 450 kyr: Implications for Marine Isotope Stage (MIS) 11. *Global and Planetary Change*, 24(1), 7–26. [https://doi.org/10.1016/S0921-8181\(99\)00069-7](https://doi.org/10.1016/S0921-8181(99)00069-7)
- Hodell, D. A., Charles, C. D., & Sierro, F. J. (2001). Late Pleistocene evolution of the ocean's carbonate system. *Earth and Planetary Science Letters*, 192(2), 109–124. [https://doi.org/10.1016/S0012-821X\(01\)00430-7](https://doi.org/10.1016/S0012-821X(01)00430-7)
- Hodell, D. A., Evans, H. F., Channell, J. E. T., & Curtis, J. H. (2010). Phase relationships of North Atlantic ice-rafted debris and surface-deep climate proxies during the last glacial period. *Quaternary Science Reviews*, 29(27–28), 3875–3886. <https://doi.org/10.1016/j.quascirev.2010.09.006>
- Hodell, D. A., Venz, K. A., Charles, C. D., & Ninnemann, U. S. (2003). Pleistocene vertical carbon isotope and carbonate gradients in the South Atlantic sector of the Southern Ocean. *Geochemistry, Geophysics, Geosystems*, 4(1), 1004. <https://doi.org/10.1029/2002GC000367>
- Hönisch, B., & Hemming, N. G. (2005). Surface ocean pH response to variations in pCO<sub>2</sub> through two full glacial cycles. *Earth and Planetary Science Letters*, 236(1–2), 305–314. <https://doi.org/10.1016/j.epsl.2005.04.027>
- Howard, W. R., & Prell, W. L. (1994). Late Quaternary CaCO<sub>3</sub> production and preservation in the Southern Ocean: Implications for oceanic and atmospheric carbon cycling. *Paleoceanography*, 9(3), 453–482. <https://doi.org/10.1029/93PA03524>
- Huybers, P., & Langmuir, C. (2009). Feedback between deglaciation, volcanism, and atmospheric CO<sub>2</sub>. *Earth and Planetary Science Letters*, 286(3–4), 479–491. <https://doi.org/10.1016/j.epsl.2009.07.014>
- Jaccard, S. L., Galbraith, E. D., Martínez-García, A., & Anderson, R. F. (2016). Covariation of abyssal Southern Ocean oxygenation and pCO<sub>2</sub> throughout the last ice age. *Nature*, 530(7589), 207–210. <https://doi.org/10.1038/nature16514>
- Jouzel, J., Masson-Delmotte, V., Cattani, O., Dreyfus, G., Falourd, S., Hoffmann, G., et al. (2007). Orbital and millennial Antarctic climate variability over the past 800,000 years. *Science*, 317(5839), 793–796. <https://doi.org/10.1126/science.1141038>
- Kanfoush, S. L., Hodell, D. A., Charles, C. D., Guilderson, T. P., Mortyn, P. G., & Ninnemann, U. S. (2000). Millennial-scale instability of the Antarctic ice sheet during the last glaciation. *Science*, 288(5472), 1815–1819. <https://doi.org/10.1126/science.288.5472.1815>
- Keigwin, L. D., & Boyle, E. A. (1999). Surface and deep ocean variability in the northern Sargasso Sea during Marine Isotope Stage 3. *Paleoceanography*, 14(2), 164–170. <https://doi.org/10.1029/1998PA0900026>
- Keigwin, L. D., & Jones, G. A. (1994). Western North Atlantic evidence for millennial-scale changes in ocean circulation and climate. *Journal of Geophysical Research*, 99(C6), 12,397–12,410. <https://doi.org/10.1029/94JC00525>
- Kerr, J., Rickaby, R., Yu, J., Elderfield, H., & Yu, A. (2017). The effect of ocean alkalinity and carbon transfer on deep-sea carbonate ion concentration during the past five glacial cycles. *Earth and Planetary Science Letters*, 471, 42–53. <https://doi.org/10.1016/j.epsl.2017.04.042>
- Key, R. M., Kozyr, A., Sabine, C. L., Lee, K., Wanninkhof, R., Bullister, J. L., et al. (2004). A global ocean carbon climatology: Results from Global Data Analysis Project (GLODAP). *Global Biogeochemical Cycles*, 18, GB4031. <https://doi.org/10.1029/2004GB002247>
- Kissel, C., Laj, C., Labeyrie, L., Dokken, T., Voelker, A., & Blamart, D. (1999). Rapid climatic variations during marine isotopic stage 3: Magnetic analysis of sediments from Nordic Seas and North Atlantic. *Earth and Planetary Science Letters*, 171(3), 489–502. [https://doi.org/10.1016/S0012-821X\(99\)00162-4](https://doi.org/10.1016/S0012-821X(99)00162-4)
- Kohfeld, K. E., & Ridgwell, A. J. (2009). Glacial-interglacial variability in atmospheric CO<sub>2</sub>. In C. Le Quééré, & E. Saltzman (Eds.), *Surface ocean—Lower atmosphere processes, Geophysical Research Series* (Vol. 187, pp. 251–286). Washington, DC: American Geophysical Union.
- Kuhn, G., & Diekmann, B. (2002). Late Quaternary variability of ocean circulation in the southeastern South Atlantic inferred from the terrigenous sediment record of a drift deposit in the southern Cape Basin (ODP Site 1089). *Palaeogeography Palaeoclimatology Palaeoecology*, 182(3–4), 287–303. [https://doi.org/10.1016/S0031-0182\(01\)00500-4](https://doi.org/10.1016/S0031-0182(01)00500-4)
- Labeyrie, L. D., Duplessy, J.-C., & Blanc, P. L. (1987). Variations in mode of formation and temperature of oceanic deep water over the past 125,000 years. *Nature*, 327(6122), 477–482. <https://doi.org/10.1038/327477a0>

- Lacerra, M., Lund, D., Yu, J., & Schmittner, A. (2017). Carbon storage in the mid-depth Atlantic during millennial-scale climate events. *Paleoceanography*, 32, 780–795. <https://doi.org/10.1002/2016PA003081>
- Le, J., & Shackleton, N. J. (1992). Carbonate dissolution fluctuations in the western equatorial Pacific during the late Quaternary. *Paleoceanography*, 7(1), 21–42. <https://doi.org/10.1029/91PA02854>
- Lewis, E., & Wallace, D. W. R. (1998). *Program developed for CO<sub>2</sub> system calculations*. Carbon Dioxide Information Analysis Center, Oak Ridge National Laboratory, US Department of Energy, Oak Ridge, TN.
- Lisiecki, L. E., & Raymo, M. E. (2009). Diachronous benthic  $\delta^{18}\text{O}$  responses during late Pleistocene terminations. *Paleoceanography*, 24, PA3210. <https://doi.org/10.1029/2009PA001732>
- Locarnini, R. A., Mishonov, A. V., Antonov, J. I., Boyer, T. P., Garcia, H. E., Baranova, O. K., et al. (2010). In S. Levitus (Ed.), *World Ocean Atlas 2009, Volume 1: Temperature, NOAA Atlas*. Washington, DC: U.S. Government Printing Office.
- Lynch-Stieglitz, J., Schmidt, M. W., Henry, L. G., Curry, W. B., Skinner, L. C., Mulitza, S., et al. (2014). Muted change in Atlantic overturning circulation over some glacial-aged Heinrich events. *Nature Geoscience*, 7(2), 144–150. <https://doi.org/10.1038/ngeo2045>
- Marchitto, T. M., Lynch-Stieglitz, J., & Hemming, S. R. (2005). Deep Pacific CaCO<sub>3</sub> compensation and glacial-interglacial atmospheric CO<sub>2</sub>. *Earth and Planetary Science Letters*, 231(3–4), 317–336. <https://doi.org/10.1016/j.epsl.2004.12.024>
- Margari, V., Skinner, L. C., Tzedakis, P. C., Ganopolski, A., Vautravers, M., & Shackleton, N. J. (2010). The nature of millennial-scale climate variability during the past two glacial periods. *Nature Geoscience*, 3(2), 127–131. <https://doi.org/10.1038/ngeo740>
- Martínez-García, A., Sigman, D. M., Ren, H., Anderson, R. F., Straub, M., Hodell, D. A., et al. (2014). Iron fertilization of the sub-Antarctic Ocean during the last ice age. *Science*, 343(6177), 1347–1350. <https://doi.org/10.1126/science.1246848>
- McManus, J. F., Francois, R., Gherardi, J., & Keigwin, L. D. (2004). Collapse and rapid resumption of Atlantic meridional circulation linked to deglacial climate changes. *Nature*, 428(6985), 834–837. <https://doi.org/10.1038/nature02494>
- Mortyn, P. G., Charles, C. D., & Hodell, D. A. (2002). Southern Ocean upper water column structure over the last 140 kyr with emphasis on the glacial terminations. *Global and Planetary Change*, 34(3–4), 241–252. [https://doi.org/10.1016/S0921-8181\(02\)00118-2](https://doi.org/10.1016/S0921-8181(02)00118-2)
- Mortyn, P. G., Charles, C. D., Ninnemann, U. S., Ludwig, K., & Hodell, D. A. (2003). Deep sea sedimentary analogs for the Vostok ice core. *Geochemistry, Geophysics, Geosystems*, 4(8), 8405. <https://doi.org/10.1029/2002gc000475>
- NGRIP members (2004). High-resolution record of Northern Hemisphere climate extending into the last interglacial period. *Nature*, 431, 147–151. <https://doi.org/10.1038/nature02805>
- Ninnemann, U. S., Charles, C. D., & Hodell, D. A. (1999). Origin of global millennial scale climate events: Constraints from the Southern Ocean deep sea sedimentary record. In P. U. Clark, R. S. Webb, & L. D. Keigwin (Eds.), *Mechanisms of global climate change at millennial time scales, Geophysical Monograph Series* (Vol. 112, pp. 99–112). Washington, DC: American Geophysical Union.
- Opdyke, B. N., & Walker, J. C. G. (1992). Return of the coral reef hypothesis: Basin to shelf partitioning of CaCO<sub>3</sub> and its effect on atmospheric CO<sub>2</sub>. *Geology*, 20(8), 733–736. [https://doi.org/10.1130/0091-7613\(1992\)020<0733:ROTCRH>2.3.CO;2](https://doi.org/10.1130/0091-7613(1992)020<0733:ROTCRH>2.3.CO;2)
- Orsi, A. H., Whitworth, T., & Nowlin, W. D. (1995). On the meridional extent and fronts of the Antarctic Circumpolar Current. *Deep Sea Research*, 42(5), 641–673. [https://doi.org/10.1016/0967-0637\(95\)00021-W](https://doi.org/10.1016/0967-0637(95)00021-W)
- Peterson, L. C., & Prell, W. L. (1985). Carbonate preservation and rates of climate change: An 800 kyr record from the Indian Ocean. In E. T. Sundquist, & W. S. Broecker (Eds.), *The carbon cycle and atmospheric CO<sub>2</sub>: Natural variations Archean to present, Geophysical Monograph Series* (Vol. 32, pp. 251–269). Washington, DC: American Geophysical Union.
- Piotrowski, A. M., Galy, A., Nicholl, J. A. L., Roberts, N., Wilson, D. J., Clegg, J. A., & Yu, J. (2012). Reconstructing deglacial North and South Atlantic deep water sourcing using foraminiferal Nd isotopes. *Earth and Planetary Science Letters*, 357, 289–297. <https://doi.org/10.1016/j.epsl.2012.09.036>
- Piotrowski, A. M., Goldstein, S. L., Hemming, S., Fairbanks, R. G., & Zylberberg, D. R. (2008). Oscillating glacial northern and southern deep water formation from combined neodymium and carbon isotopes. *Earth and Planetary Science Letters*, 272(1–2), 394–405. <https://doi.org/10.1016/j.epsl.2008.05.011>
- Ridgwell, A., & Zeebe, R. E. (2005). The role of the global carbonate cycle in the regulation and evolution of the Earth system. *Earth and Planetary Science Letters*, 234(3–4), 299–315. <https://doi.org/10.1016/j.epsl.2005.03.006>
- Ridgwell, A. J. (2001). *Glacial-interglacial perturbations in the global carbon cycle*. PhD thesis, University of East Anglia at Norwich (UK).
- Ridgwell, A. J., Watson, A. J., Maslin, M. A., & Kaplan, J. O. (2003). Implications of coral reef buildup for the controls on atmospheric CO<sub>2</sub> since the Last Glacial Maximum. *Paleoceanography*, 18(4), 1083. <https://doi.org/10.1029/2003PA000893>
- Roberts, J., Gottschalk, J., Skinner, L. C., Peck, V. L., Kender, S., Elderfield, H., et al. (2015). Evolution of South Atlantic density and chemical stratification across the last deglaciation. *Proceedings of the National Academy of Sciences of the United States of America*, 113(3), 514–519. <https://doi.org/10.1073/pnas.1511252113>
- Sachs, J. P., & Anderson, R. F. (2003). Fidelity of alkenone paleotemperatures in southern Cape Basin sediment drifts. *Paleoceanography*, 18(4), 1082. <https://doi.org/10.1029/2002PA000862>
- Schmittner, A., & Galbraith, E. D. (2008). Glacial greenhouse-gas fluctuations controlled by ocean circulation changes. *Nature*, 456(7220), 373–376. <https://doi.org/10.1038/nature07531>
- Shackleton, N. J. (1967). Oxygen isotope analyses and Pleistocene temperatures re-assessed. *Nature*, 215(5096), 15–17. <https://doi.org/10.1038/215015a0>
- Siddall, M., Rohling, E. J., Thompson, W. G., & Waelbroeck, C. (2008). Marine Isotope Stage 3 sea level fluctuations: Data synthesis and new outlook. *Reviews of Geophysics*, 46, RG4003. <https://doi.org/10.1029/2007RG000226>
- Sigman, D. M., & Boyle, E. A. (2000). Glacial/interglacial variations in atmospheric carbon dioxide. *Nature*, 407(6806), 859–869. <https://doi.org/10.1038/35038000>
- Sigman, D. M., McCorkle, D. C., & Martin, W. R. (1998). The calcite lysocline as a constraint on glacial/interglacial low-latitude production changes. *Global Biogeochemical Cycles*, 12(3), 409–427. <https://doi.org/10.1029/98GB01184>
- Skinner, L. C., Elderfield, H., & Hall, M. (2007). Phasing of millennial climate events and Northeast Atlantic Deep-Water temperature change since 50 Ka BP. In A. Schmittner, J. C. H. Chiang, & S. R. Hemming (Eds.), *Ocean circulation: Mechanisms and impacts, Geophysical Monograph Series* (pp. 197–208). Washington, DC: American Geophysical Union.
- Skinner, L. C., Fallon, S., Waelbroeck, C., Michel, E., & Barker, S. (2010). Ventilation of the deep Southern Ocean and deglacial CO<sub>2</sub> rise. *Science*, 328(5982), 1147–1151. <https://doi.org/10.1126/science.1183627>
- Skinner, L. C., & Shackleton, N. J. (2005). An Atlantic lead over Pacific deep-water change across Termination I: Implications for the application of the marine isotope stage stratigraphy. *Quaternary Science Reviews*, 24(5–6), 571–580. <https://doi.org/10.1016/j.quascirev.2004.11.008>
- Skinner, L. C., Waelbroeck, C., Scrivner, A. E., & Fallon, S. J. (2014). Radiocarbon evidence for alternating northern and southern sources of ventilation of the deep Atlantic carbon pool during the last deglaciation. *Proceedings of the National Academy of Sciences of the United States of America*, 111(15), 5480–5484. <https://doi.org/10.1073/pnas.1400668111>

- Sokolov, S., & Rintoul, S. R. (2009). Circumpolar structure and distribution of the Antarctic Circumpolar Current fronts: 2. Variability and relationship to sea surface height. *Journal of Geophysical Research*, *114*, C11018. <https://doi.org/10.1029/2008JC005108>
- Sosdian, S. M., Rosenthal, Y., & Toggweiler, J. R. (2018). Deep Atlantic carbonate ion and CaCO<sub>3</sub> compensation during the ice ages. *Paleoceanography and Paleoclimatology*, *33*. <https://doi.org/10.1029/2017PA003312>
- Stoner, J. S., Channell, J. E. T., Hodell, D. A., & Charles, C. D. (2003). A ~580 kyr paleomagnetic record from the sub-Antarctic South Atlantic (Ocean Drilling Program Site 1089). *Journal of Geophysical Research*, *108*(B5), 2244. <https://doi.org/10.1029/2001JB001390>
- Stramma, L., & England, M. (1999). On the water masses and mean circulation of the South Atlantic Ocean. *Journal of Geophysical Research*, *104*(C9), 20,863–20,883. <https://doi.org/10.1029/1999JC900139>
- Talley, L. D. (2013). Closure of the global overturning circulation through the Indian, Pacific, and Southern Oceans: Schematics and transports. *Oceanography*, *26*(1), 80–97. <https://doi.org/10.5670/oceanog.2013.07>
- Thornalley, D. J. R., Barker, S., Becker, J., Hall, I. R., & Knorr, G. (2013). Abrupt changes in deep Atlantic circulation during the transition to full glacial conditions. *Paleoceanography*, *28*, 253–262. <https://doi.org/10.1002/palo.20025>
- Thunell, R. C. (1982). Carbonate dissolution and abyssal hydrography in the Atlantic Ocean. *Marine Geology*, *47*(3–4), 165–180. [https://doi.org/10.1016/0025-3227\(82\)90067-6](https://doi.org/10.1016/0025-3227(82)90067-6)
- Toggweiler, J. R. (1999). Variation of atmospheric CO<sub>2</sub> by ventilation of the ocean's deepest water. *Paleoceanography*, *14*(5), 571–588. <https://doi.org/10.1029/1999PA900033>
- Trauth, M. H. (2013). TURBO2: A MATLAB simulation to study the effects of bioturbation on paleoceanographic time series. *Computational Geosciences*, *6*(1), 1–10. <https://doi.org/10.1016/j.cageo.2013.05.003>
- Tschumi, T., Joos, F., Gehlen, M., & Heinze, C. (2011). Deep ocean ventilation, carbon isotopes, marine sedimentation and the deglacial CO<sub>2</sub> rise. *Climate of the Past*, *7*(3), 771–800. <https://doi.org/10.5194/cp-7-771-2011>
- Tucholke, B. E., & Embley, R. W. (1984). Cenozoic regional erosion of the abyssal sea floor off South Africa. In J. S. Schlee (Ed.), *Interregional unconformities and hydrocarbon accumulation, American Association of Petroleum Geologists Special Publication* (Vol. 36, pp. 145–164). Tulsa, OK.
- Veres, D., Bazin, L., Landais, A., Toyé Mahamadou Kele, H., Lemieux-Dudon, B., Parrenin, F., et al. (2013). The Antarctic ice core chronology (AICC2012): An optimized multi-parameter and multi-site dating approach for the last 120 thousand years. *Climate of the Past*, *8*(6), 6011–6049. <https://doi.org/10.5194/cpd-8-6011-2012>
- Waelbroeck, C., Labeyrie, L., Michel, E., Duplessy, J. C., McManus, J. F., Lambeck, K., et al. (2002). Sea-level and deep water temperature changes derived from benthic foraminifera isotopic records. *Quaternary Science Reviews*, *21*(1–3), 295–305. [https://doi.org/10.1016/S0277-3791\(01\)00101-9](https://doi.org/10.1016/S0277-3791(01)00101-9)
- Wall-Palmer, D., Hart, M. B., Smart, C. W., Sparks, R. S. J., Le Friant, A., Boudon, G., et al. (2012). Pteropods from the Caribbean Sea: Variations in calcification as an indicator of past ocean carbonate saturation. *Biogeosciences*, *9*(1), 309–315. <https://doi.org/10.5194/bg-9-309-2012>
- Weltje, G. J., & Tjallingii, R. (2008). Calibration of XRF core scanners for quantitative geochemical logging of sediment cores: Theory and application. *Earth and Planetary Science Letters*, *274*(3–4), 423–438. <https://doi.org/10.1016/j.epsl.2008.07.054>
- Yu, J., Anderson, R. F., Jin, Z., Menviel, L., Zhang, F., Ryerson, F. J., & Rohling, E. J. (2014). Deep South Atlantic carbonate chemistry and increased interocean deep water exchange during last deglaciation. *Quaternary Science Reviews*, *90*, 80–89. <https://doi.org/10.1016/j.quascirev.2014.02.018>
- Yu, J., Anderson, R. F., Jin, Z., Rae, J. W. B., Opdyke, B. N., & Eggins, S. M. (2013). Responses of the deep ocean carbonate system to carbon reorganization during the last glacial-interglacial cycle. *Quaternary Science Reviews*, *76*, 39–52. <https://doi.org/10.1016/j.quascirev.2013.06.020>
- Yu, J., Broecker, W. S., Elderfield, H., Jin, Z., McManus, J., & Zhang, F. (2010). Loss of carbon from the deep sea since the Last Glacial Maximum. *Science*, *330*(6007), 1084–1087. <https://doi.org/10.1126/science.1193221>
- Yu, J., Elderfield, H., & Piotrowski, A. M. (2008). Seawater carbonate ion- $\delta^{13}\text{C}$  systematics and application to glacial-interglacial North Atlantic Ocean circulation. *Earth and Planetary Science Letters*, *271*(1–4), 209–220. <https://doi.org/10.1016/j.epsl.2008.04.010>
- Yu, J., Menviel, L., Jin, Z. D., Thornalley, D. J. R., Barker, S., Marino, G., et al. (2016). Sequestration of carbon in the deep Atlantic during the last glaciation. *Nature Geoscience*, *9*(4), 319–324. <https://doi.org/10.1038/ngeo2657>
- Yu, J., Thornalley, D. J. R., Rae, J. W. B., & McCave, N. I. (2013). Calibration and application of B/Ca, Cd/Ca, and  $\delta^{11}\text{B}$  in *Neogloboquadrina pachyderma* (sinistral) to constrain CO<sub>2</sub> uptake in the subpolar North Atlantic during the last deglaciation. *Paleoceanography*, *28*, 237–252. <https://doi.org/10.1002/palo.20024>